VOLUME II ISSUE II

CANADIAN JOURNAL OF UNDERGRADUATE RESEARCH

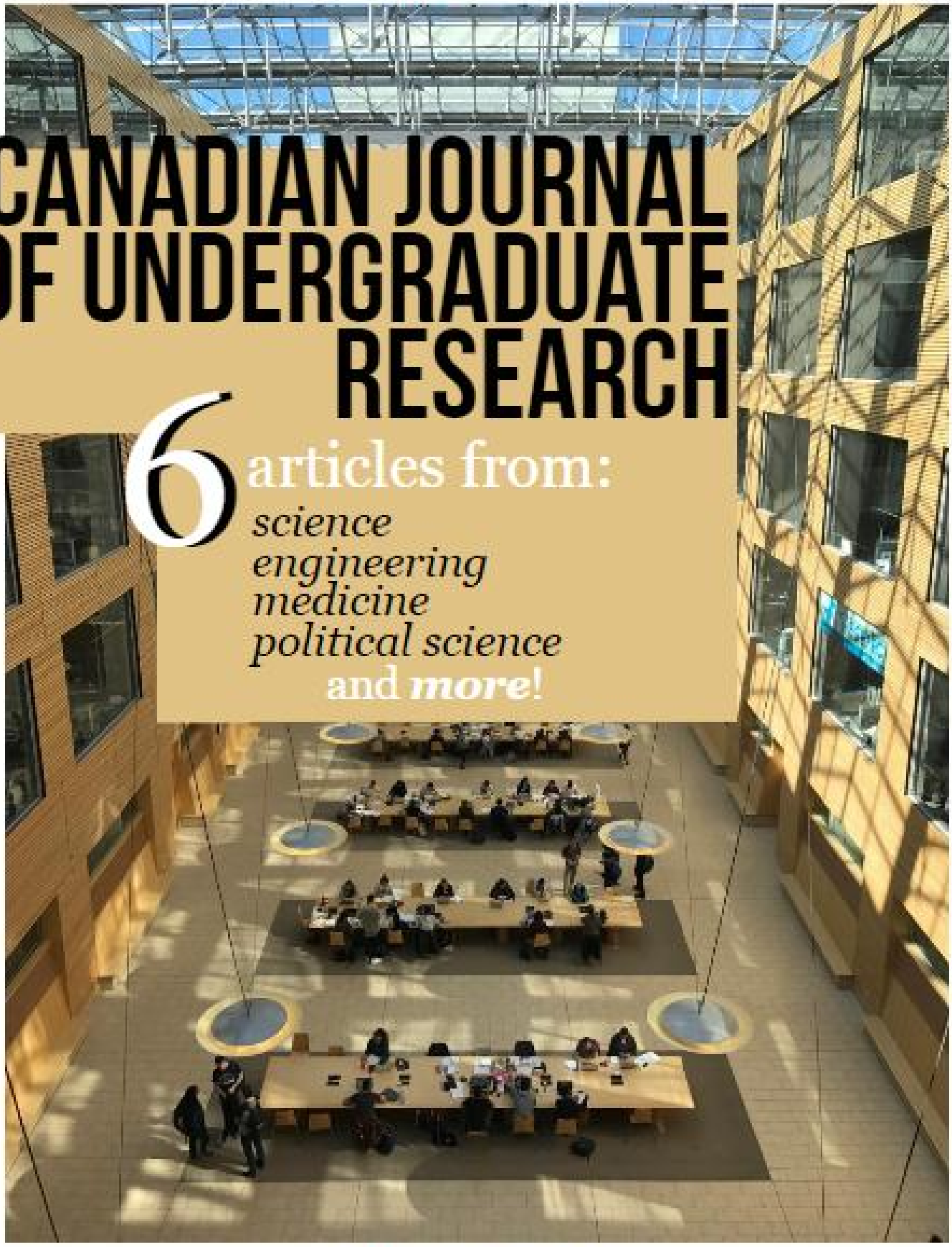

6 articles from:

science
engineering
medicine
political science
and ***more***!

AUGUST 2017

TABLE OF CONTENTS

EDITORIAL BOARD

LETTER FROM THE EDITORS

CJUR was founded in April 2016 with the goal of empowering undergraduate researchers by providing them with the opportunity to share their research with their peers and develop their academic writing skills. Since our first issue, we have observed a steady increase in both the number and diversity of submissions received, and we hope to continue to expand the journal's outreach throughout the upcoming issues. Furthermore, we hope to motivate and inspire undergraduates who are considering research by highlighting the accomplishments of their peers across a diverse range of disciplines.

In this issue, we feature submissions from the University of British Columbia, Vancouver Island University, and University of Toronto Mississauga. This issue covers a range of topics which span the disciplines of psychology, computer science, biology, physics, mathematics, and gender studies. We hope you will join us in celebrating the accomplishments of the 9 undergraduate authors that contributed to this issue.

Sincerely,
Editorial Team at the Canadian Journal of Undergraduate Research

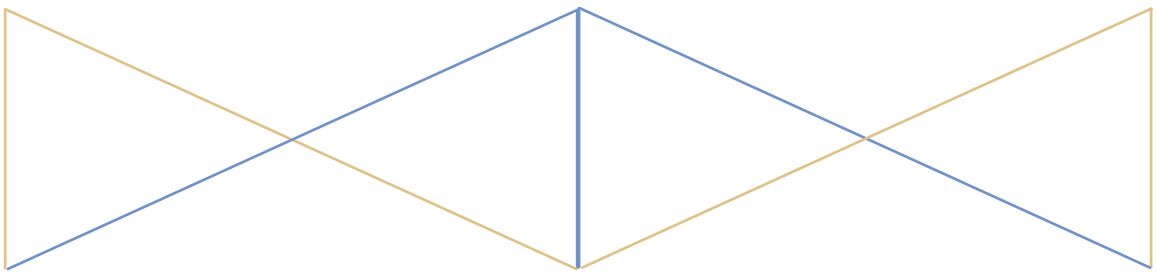

High Voltage Phenomena In Rarefied Air: A DIY Approach

Frank Fang Jia, Georgiy Maruzhenko
University of British Columbia, Vancouver, British Columbia, Canada

Abstract

The present experiment aims to recreate and analyze known behavior of high-voltage gaps in a near vacuum with low-cost equipment. It has been previously observed that the application of high voltages in rarified gas results in electrical breakdown and corona discharge, characterized by the production of observable plasma in the experimental area. The current study aims to identify and document a do-it-yourself (DIY) method for producing and containing electrical discharge. Further, the requirements of electrical phenomena were recorded in terms of voltage and pressure to be compared to previous models, namely Paschen's Law, as a measure of accuracy (Berzak et al., 2006). The operating experimental apparatus was demonstrated to exhibit the same discharge phenomena as previously recorded (Peek, 1929). New models for voltage and pressure requirements for electrical breakdown and corona discharge were produced. Literature comparison was available for the voltage model of electrical breakdown, where significant difference was identified between Paschen's model and current data. The present study may contribute further evidence to the inadequacy of Paschen's law in describing breakdown voltages at high pressure-distance configurations.

Introduction

From antique CRT televisions to high-tech ion thrusters, electrical discharge, or a lack thereof, is critical for the operation of modern machinery. Precise control of electrical arcs is thus a fundamental requirement of present day technology, justifying further research on the topic.

The current model for electrical phenomena is based upon the dielectric strength of air (Peek, 1929). At lower voltages, the electric field across two electrodes is sufficiently low for air to act as an insulator. There is no conductance and no electric arc is observed.

As voltage is increased, increased dielectric flux density around the conductors forces the surrounding air to become conductive, forming a film of purple plasma around the active electrodes, named corona discharge (Peek, 1929; Goldman et al., 1985). However, the electrode gap is not yet fully conductive, so no arc is created.

Electrical breakdown occurs when the dielectric strength of the air gap is exceeded. At this voltage, the neutral air molecules in the gap are ionized by the high potential difference, and the air becomes a sea of conductive charges (Bawagan, 1997). At this point, the circuit is completed between the two electrodes, resulting in a bright electrical arc.

The voltage-pressure requirements for electrical discharge is predicted by Paschen's law. Recent experimental evidence has both supported and disputed the accuracy of this model (Lisovskiy et al., 2000; Berzak et al., 2006; Massarcyzk et al., 2016). The current experiment aims to gather further experimental evidence for previously proposed models for electrical breakdown and to produce a novel model fit for the requirements of corona discharge. This study also aims to determine whether a DIY approach to the experimental apparatus is able to yield viable data.

Methods

Measurement Apparatus

A compact fluorescent lamp (CFL) ballast was connected to a flyback transformer to convert AC into high voltage (HV) DC. The input of the ballast is connected to a power cord, and the output to the flyback transformer.The output of the flyback transformer served as one electrode, and the ground as the other.

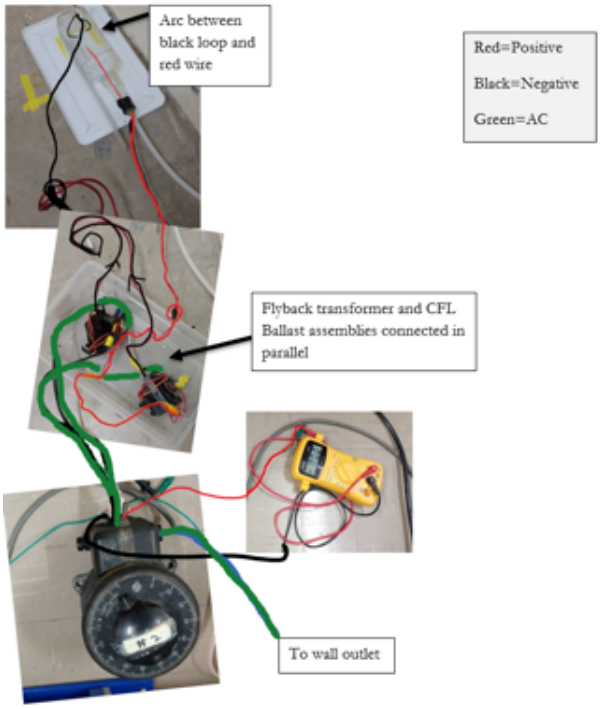

Fig. 1. Experimental apparatus wiring illustration

Two transformers were connected in parallel and plugged into a variac that controlled input AC voltage (VAC).

The vacuum chamber was composed of glass with a 3/8" hole at one end drilled using a ceramic spade bit. A wire bent into a loop of diameter 5cm was inserted and the hole sealed with hot glue to prevent vacuum leaks. The other end of the chamber was held closed by a rubber stopper with a 1/4" hose barb. A wire was attached to the hose barb to act as a point of conduction.

A vacuum pump with a connected 1/4" hose barb was used. A cross with four female NPT threads connected two hose barbs as well as a pressure bleed valve and a vacuum gauge.

Measurements

Corona Discharge Voltage Measurements

Upon reaching an absolute pressure of 11kPa, the input VAC was increased until a glow at the electrodes was observed. The input voltage at which this occurred was recorded. This measurement was performed with both electrode configurations at different electrode gap lengths.

Breakdown Voltage Measurements

Breakdown voltage was defined as the voltage at which an arc is struck between the two electrodes. A pressure of 17kPa was obtained and the input voltage increased until a visible arc was observed. The input voltage at which an arc was observed was recorded. This measurement was performed with both electrode configurations at different electrode gap lengths.

Breakdown Pressure Measurements

Breakdown pressure was defined as the pressure at which an arc is struck between the electrodes at a maximum input of roughly 130VAC (4500VDC). The pressure at which a visible arc is observed was recorded. This measurement was performed with both electrode configurations at different electrode gap lengths.

Results

Indicators of Phenomena

As previously indicated in literature, corona discharge was observed prior to full electrical breakdown. This glow persisted throughout the entire operation of the experimental apparatus.

When electrical breakdown occurred, the observable arc extended from only one electrode. This phenomenon was consistent with previous experiments and featured distinct on/off behavior.

Equipment Calibration

The following fit was found between DC output voltage (VDC) and AC input voltage (VAC):

$$VDC = 48.24 \cdot VAC - 1945.2. \quad (1)$$

To obtain the aforementioned fit, DC voltage output was measured for a given AC voltage input. Unfortunately, a high voltage probe was not available, so a traditional multimeter was employed for the task. This equipment was rated for 2000VDC, and so our measurement range was confined by this upper boundary. Further, the transformers were found to spike in output at a certain threshold input, thus defining a lower boundary at approximately 1800VDC. This meant that the possible range of measurements was extremely limited, and thus the fit cannot be said to be very accurate.

The HV power supplies were measured individually and a linear fit was extrapolated from the data. This individual measurement was needed as the linked power supplies produced a compounding effect that made measurement in the 1800-2000VDC range extremely

difficult. Note that in the current configuration, the power supplies are linked to double amperage rather than to double voltage, so individual measurement can be justified.

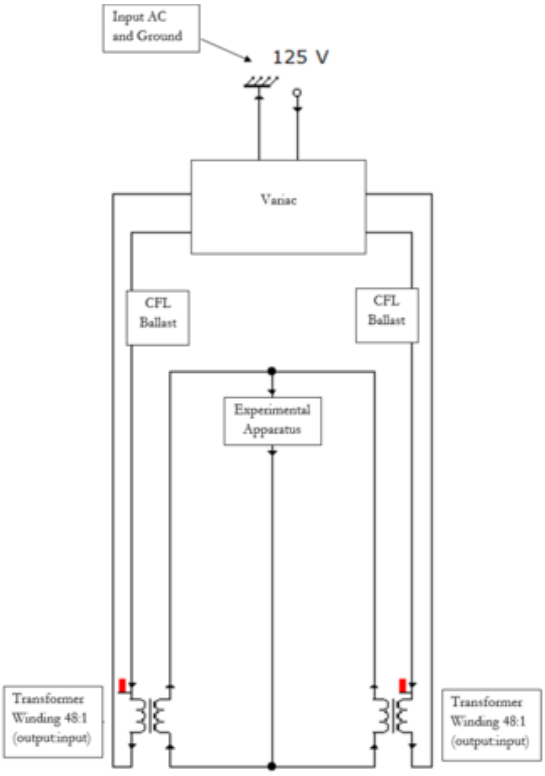

Fig. 2. Wiring diagram for the operating HV power supply

Corona Discharge Voltage Measurements (n=100)

Corona discharge measurements were performed at an absolute pressure of 10kPa and was also observed to display distinct on/off behavior. The data was able to be fitted with a linear model:

$$VDC_{Corona\ Discharge} = 13951\frac{V}{m} \cdot Gap\ Distance\ (m) + 852V. \quad (2)$$

Uncertainties for the current model were also evaluated. The final values for the slope and y-intercept were determined to be $13951 \pm 843\frac{V}{m}$ and $852 \pm 38V$, respectively. Residuals and a chi-squared value of 13.3 were calculated, indicating a less than adequate fit between the linear model and experimental data, which was also seen in the slight upward trend in the residuals plot of figure 10. However, no other model was able to produce a lower chi-squared.

The data in figure 9 show that corona voltage increases as the electrode gap distance increases. This increase ranges just under 2000VDC for a 0.1m increase in electrode gap distance. In figure 9, the calculated standard deviation was seen to be relatively small; this is supported by the fact that corona discharge displayed very distinguishable on/off behavior. However, the spread of the data points at similar electrode distances is large compared to the individual SD's. This contributes to the high chi-squared and suggests that experimental data differed significantly between trials. The source of this variation could be linked to the DIY nature of the current experiment. A slight change in the curvature in the electrodes may influence the true electrode gap, thus yielding different values for corona discharge.

Breakdown Voltage Measurements (n=131)

Clear on/off behavior was observed, but only under certain configurations. Unfortunately, the reverse electrode configuration presented difficulties for the current measurement as the arc was distributed along the circumference of the electrode loop.

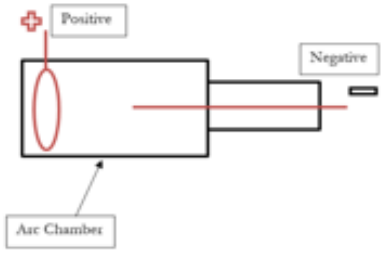

Fig. 3. Reverse electrode configuration

It was thus difficult to distinguish between corona discharge, which is present at voltages lower than the breakdown voltage, and the point of breakdown. Nevertheless, a linear model was found with the parameters $m = 20166 \pm 1332\frac{V}{m}$ and $b = 2064 \pm 58V$:

$$VDC_{Electrical\ Breakdown} = 20166\frac{V}{m} \cdot Gap\ Distance\ (m) + 2064V. \quad (3)$$

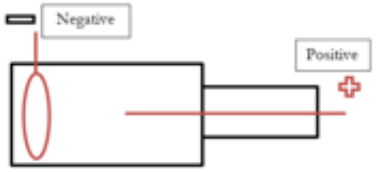

Fig.4. Normal electrode configuration. Arcing occurs between the two electrodes.

The difficulty in data collection yielded a much higher standard deviation than in corona discharge trials, as shown in figure 11. Consequently, chi-squared was quite low, at 0.56. Scattered residuals

and the aforementioned chi-squared indicate that the current linear fit is adequate.

Similar to corona discharge voltage, breakdown voltage appears to increase with increasing electrode distance. Variation between data sets is once again demonstrated to be significant. In this case, data-sets demonstrated similar slopes but vastly different Y-intercepts, ranging from 1000 VDC to 3000 VDC. These differences among experimental trials could again be attributed to the low-cost nature of the current project. Unaccounted extraneous variables, such as ambient humidity and temperature, could cause the recorded differences. Further, the output of the power supply may have fluctuated, rendering the initial VAC to VDC fit inaccurate.

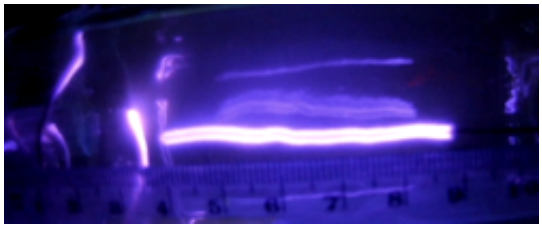

Fig. 7. Corona discharge observed at high vacuums (10kPa). Notice the lack of an arc.

Fig. 8. Observed electrical breakdown between two electrodes.

Breakdown Pressure Measurements (n=105)

Distinct on/off behavior allowed for the precise measurement of required breakdown pressure. No difficulty in distinguishing breakdown pressure was noted. Once again, a linear model was shown to be fitting for the representation of the current data. A fit was calculated with $m = -370\frac{kPa}{m} \pm 10\text{kPa}$ and $b = 42.1 \pm 0.5\text{kPa}$:

$$Pressure_{Electrical\ Breakdown} = -370\frac{kPa}{m} \cdot Gap\ Distance\ (m) + 42.1kPa. \quad (4)$$

Residuals in figure 14 demonstrate a good model fit with points evenly dispersed across the x-axis. However, a chi-squared value of 66 indicates a poor fit between data and model. In this set of experiments, data from trials were dispersed in magnitude – no distinct separation of trials was seen as per the graph of breakdown voltage versus electrode gap distance. Instead, each data set fluctuated significantly around the computed model. This observation could be the result of the relative inaccuracy of the present system. A pressure release valve was manually operated to maintain a given pressure. As such, breakdown pressure could not have been recorded with great accuracy. However, a low standard deviation, as shown on figure 13, suggests that the previous notion is not true.

A decreasing relationship was nevertheless observed in figure 13. As the electrode distance increased, the absolute pressure required for discharge decreased. Across an electrode gap difference of 0.1m, a decrease of up to 40kPa was observed to induce electrical breakdown. Figure 13 seems to be indicative of a logarithmic relationship, but a computed model did not improve the quality of the model fit. Thus, a linear relationship was found to be adequate.

Discussion

In the current experiment, linear fits were found for all voltage and pressure measurements. Phenomena with voltage as a function of electrode gap distance exhibited an increasing trend. Similarly, vacuum needed to sustain an arc increased with increasing gap distance, resulting in the negative correlation between absolute pressure and electrode gap. The obtained models are summarized as follows:

$$VDC_{Corona\ Discharge} = 13951\frac{V}{m} \cdot Gap\ Distance\ (m) + 852V. \quad (5)$$

$$VDC_{Electrical\ Breakdown} = 20166\frac{V}{m} \cdot Gap\ Distance\ (m) + 2064V. \quad (6)$$

$$Pressure_{Electrical\ Breakdown} = -370\frac{kPa}{m} \cdot Gap\ Distance\ (m) + 42.1kPa. \quad (7)$$

Voltage-Distance Analyses

As previously mentioned, corona discharge and electrical breakdown operate by the same mechanism. The key difference between the two phenomena lies in the fact that the air gap between electrodes is partially conductive at the corona voltage and completely conductive at the breakdown voltage (Goldman et al., 1985; Peek, 1929).

A positively correlated trend for voltage phenomena is intuitive when the current model of

conduction is considered. At the breakdown electric field, neutral molecules in the air gap between the electrodes are ionized. It is hypothesized that the breakdown electric field is constant regardless of gap distance, as it is known that the unit dielectric strength of air is constant at a constant pressure (Peek, 1929); this hypothesis is in fact supported by an earlier study on this topic (Lisovskiy et al., 2000). The current experimental data aligns with this theory: as electrode gap increases, more potential difference is needed to create the same electric field. Unfortunately, the current experimental apparatus is composed of a conductive loop and a piece of straight wire, and thus does not behave like an ideal plane-plane or sphere-sphere configuration, so the electric field behaves with an unknown distance dependence.

The increasing trend of corona discharge can be explained by an argument similar to the one above. Although corona phenomena result from the ionization of air surrounding an electrode, a certain threshold electric field must be present to induce this conductivity.

Comparison of the discharge and corona models yields an observable difference in slopes and y-intercepts. In both cases, the breakdown voltage model exhibits a greater value than the corona voltage plot. A t-score of 4 was calculated between the slopes of the models and a score of 17 for the y-intercepts, suggesting that both parameters are statistically different.

As corona discharge does not require complete conduction in air, it is presumed that less potential, and thus less electric field, is required to produce these effects (Goldman et al., 1985). This theory would explain the larger potentials needed to induce electrical breakdown, and is consistent with previous descriptions of corona discharge as a pre-cursor to dielectric breakdown (Peek, 1929).

The difference in slopes reveal that the voltage required for electrical breakdown increases at a greater rate than that for corona discharge. However, previous characterization of these phenomena does not fully support this finding. Although a t-score of four is often enough to distinguish the difference between two values, the relatively low t-score could suggest that the two slope values are in tension. As such, no conclusive comparison can be established with current data.

Pressure-Distance Analysis

In the given model, there exists a negative correlation between pressure and gap length. Pressures above the breakdown pressure would contain a too-high density of air for dielectric breakdown. Ionization of air in the gap would thus be not possible, and no spark was created. This is supported by the positively correlated linear behavior of dielectric strength with increasing absolute pressure, as established by Peek in 1929. So, higher absolute pressure results in higher dielectric strength, thus requiring shorter electrode distances for an arc to occur at the same input voltage.

Comparison of Electrode Configurations

The current data suggests that electrode configuration is not a factor in electrical breakdown. Average t-scores were calculated to be 0.54, 0.56, and 0.28 between data for the different electrode configurations.

Comparison to Literature

The currently accepted model for electrical breakdown in a vacuum is mathematically described by Paschen's law (Berzak et al., 2006; Wang, 2013; Massarczyk et al., 2016; Peek, 1929):

$$V_{breakdown} = \frac{Bpd}{\ln(Apd) - \ln\left[\ln\left(1+\frac{1}{\gamma_{se}}\right)\right]} \quad (8)$$

$V_{breakdown}$ represents the voltage required for discharge to occur. P and d signify the pressure in kilopascals and electrode gap in centimeters, respectively. A and B are experimentally determined constants with units $(kPa \times cm)^{-1}$.

Previous analyses were conducted with breakdown voltage as the y-axis and the product of pressure and electrode gap distance as the x-axis, as displayed in figure 15 (Al-Hakary et al., 2014; Berzak et al., 2006).

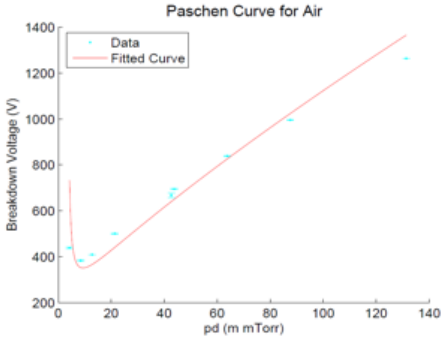

Figure 15. Experimental Paschen's curve for air. Taken without permission from Berzak et al., 2006.

In the present study, a linear correlation is expected as either pressure or electrode gap distance increases. This is because the non-linear dip in breakdown voltage seen in figure 15 is far below the operating conditions of the current experiment. This supports our current findings – breakdown voltage increases linearly with increasing electrode gap distance and increasing pressure.

It must be noted that the great majority of experiments conducted to verify Paschen's law were operated in much lower pressures than those used in the present study. In the experiment that produced figure 15, the pressures used were on the 10-1kPa magnitude (Berzak et al., 2006). The current experiment explored pressures in the 101kPa magnitude. To explore whether breakdown voltage at higher pressures, and thus higher pressure-distance x-values, is consistent with Paschen's law, our current model was plotted with other available experimental data in figure 16 and 17.

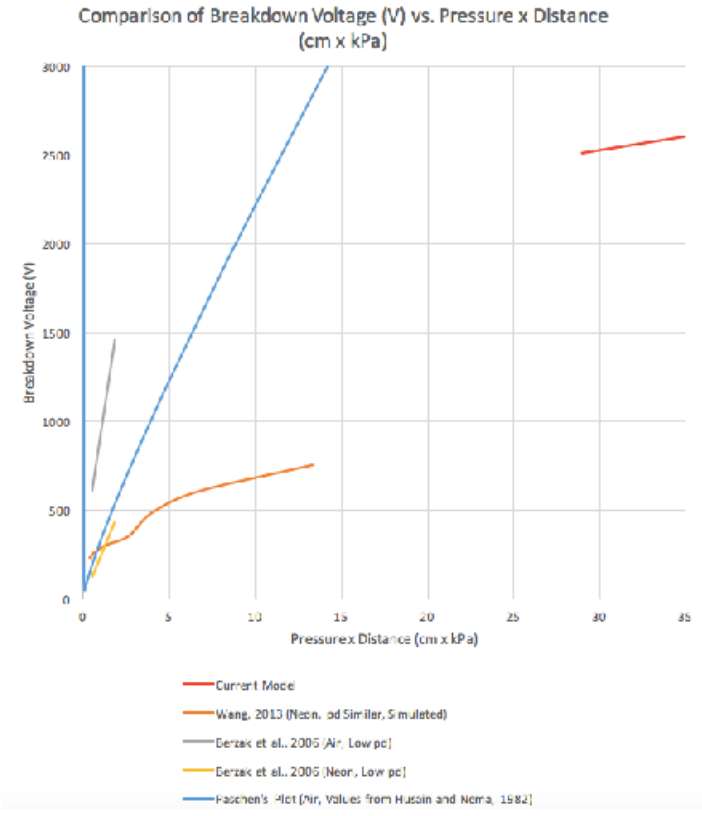

Fig. 16. Comparison of current model with literature data and mathematical models in their respective pressure-distance ranges. Model fits were calculated from raw data taken without permission from the mentioned research papers.

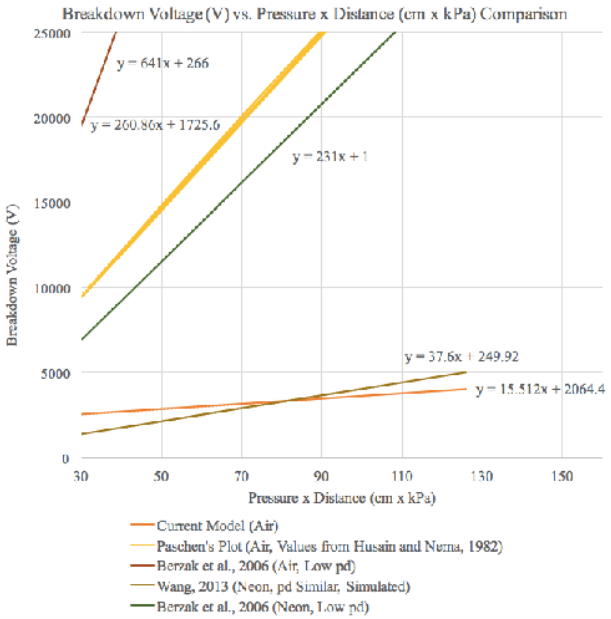

Fig. 17. Comparison of current model with literature data and mathematical models with extrapolated slopes for direct comparison. Model fits were calculated from raw data taken without permission from the mentioned research papers.

From the figures, it is clear that there exists immense variation in current experimental data. Specifically, experiments involving low pressure-distance configurations were modeled by slopes much greater than the present fit. A calculated chi-squared between the Paschen's law model and our current data yielded a value on the order of 1017 magnitude, indicating an obvious difference between the two fits. Previous experiments with similar experimental conditions as the current experiment, however, were able to produce plots on or near the same order of magnitude as our current data, but unfortunately did not involve air as a conductive medium (Wang, 2013; Massarczyk et al., 2016).

To create a point of reference, data for neon and air environments were taken from Berzak et al.'s 2006 study of Paschen's law. In their study, low pressure-distance configurations were used, on the 10-1kPa magnitude as previously mentioned. The slopes of both plots lie in the same order of magnitude as a mathematically calculated plot of Paschen's law, but are significantly greater than that produced by the current study. Wang's 2013 simulation in neon, on the other hand, involved conditions more similar to the present experiment and produced a plot on the

same order of magnitude as our current model. This comparison suggests that voltage versus pressure-distance behavior assumes a lower slope for higher pressure-distance values, and that Paschen's law is inadequate for describing higher pressure-distance configurations.

Given the DIY nature of the current experiment, however, this finding is not conclusive. Thus, there are two possible explanations for the gathered data. First, the DIY experimental apparatus and measuring techniques employed in the current experiment was insufficient in gathering accurate data. Second, the current Paschen's model breaks down at the pressure distance values tested in the current study.

Conclusion

In the current experiment, an experimental apparatus was built to observe and record the nature of high voltage phenomena in a near-vacuum. Three main classes of measurements were conducted: corona discharge voltage, electrical breakdown voltage, and electrical breakdown pressure. The gathered data was fitted to find a linear relationship between the phenomena voltage and electrode gap length:

$$VDC_{Corona\ Discharge} = 13951\frac{V}{m} \cdot Gap\ Distance\ (m) + 852V. \quad (9)$$

$$VDC_{Electrical\ Breakdown} = 20166\frac{V}{m} \cdot Gap\ Distance\ (m) + 2064V. \quad (10)$$

The absolute pressure needed for arcing to occur was found to decrease linearly with increasing electrode

$$Pressure_{Electrical\ Breakdown} = -370\frac{kPa}{m} \cdot Gap\ Distance\ (m) + 42.1kPa. \quad (11)$$

Previous experimental models were not found for corona discharge voltage and electrical breakdown pressure requirements. However, an established model, Paschen's law, was available to predict the breakdown voltage of a given configuration as a function of pressure times distance. The current experimental model was compared to the mathematical model as well as available research on the topic. It was found that the current DIY apparatus could be insufficient in yielding viable data. However, the current findings also reveal the possibility that Paschen's law is not adequate in predicting electrical breakdown voltage at higher pressure-distance configurations.

References

Al-Hakary, S. K., Dosky, L., & Talal, S. K. (2014). Investigation of Hot Cathode and Hollow Anode of Argon Glow Discharge Plasma. Applied Physics Research, 6(5). doi:10.5539/apr.v6n5p45

Bawagan, A. (1997). A stochastic model of gaseous dielectric breakdown. Chemical Physics Letters, 281(4-6), 325-331. doi:10.1016/s0009-2614(97)01192-5

Berzak, L.F., Dorfman, S. E., & Smith, S. P. (2006). Paschen's law in air and noble gases.

Emeleus, K. G. (1982). Anode glows in glow discharges: outstanding problems. International Journal of Electronics, 52(5), 407-417. doi:10.1080/00207218208901448

Geissler Tubes. (2006). Retrieved March 12, 2017, from http://lrrpublic.cli.det.nsw.edu.au/lrrSecure/Sites/Web/physics_explorer/physics/lo/cathode_07/cathode_07_01.htm

Goldman, M., Goldman, A., & Sigmond, R. S. (1985). The corona discharge, its properties and specific uses. Pure and Applied Chemistry, 57(9). doi:10.1351/pac198557091353

Husain, E., & Nema, R. S. (1982). Analysis of Paschen Curves for air, N2 and SF6 Using the Townsend Breakdown Equation. IEEE Transactions on Electrical Insulation, EI-17(4), 350-353. doi:10.1109/tei.1982.298506

Li, X., Cui, X., Lu, T., Li, D., Chen, B., & Fu, Y. (2016). Influence of air pressure on the detailed characteristics of corona current pulse due to positive corona discharge. Physics of Plasmas, 23(12), 123516. doi:10.1063/1.4971804

Lisovskiy, V. A., Yakovin, S. D., & Yegorenkov, V. D. (2000). Low-pressure gas breakdown in uniform dc electric field. Journal of Physics D: Applied Physics, 33(21), 2722-2730. doi:10.1088/0022-3727/33/21/310

Massarczyk, R., Chu, P., Elliott, S. R., Rielage, K., Dugger, C., & Xu, W. (2015). Paschen's law studies in cold gases. Retrieved from https://arxiv.org/abs/1612.07170v1

Peek, F. W. (1929). Dielectric Phenomena in High Voltage Engineering (3rd ed.). New York, NY: McGraw-Hill Book Company, inc.

Wang, J. (2013). Simulation of Gas Discharge in Tube and Paschen's Law. Optics and Photonics Journal, 03(02), 313-317. doi:10.4236/opj.2013.32b073

Xiao, D. (2016). Gas discharge and gas insulation. Heidelberg: Springer.

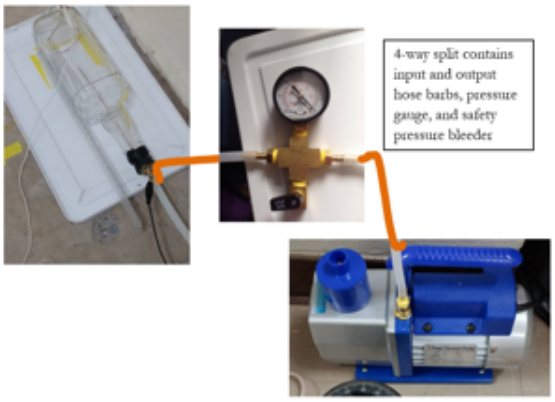

Fig. 5. Airflow apparatus for the present experiment

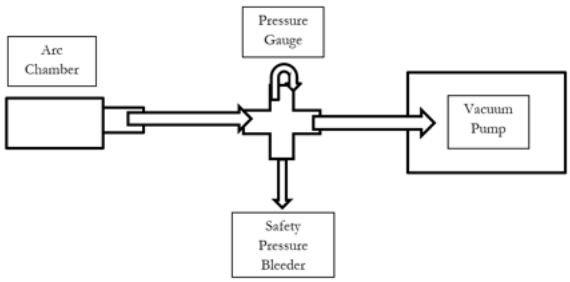

Fig. 6. Airflow diagram

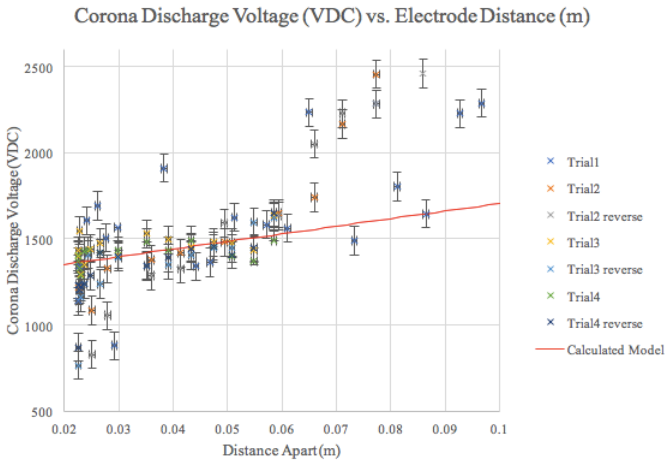

Fig. 9. Corona voltage data with fitted model. Uncertainties calculated from SD.

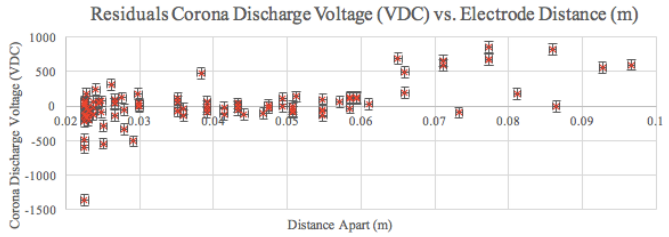

Fig. 10. Residuals of the calculated model. Notice the lack of a clear trend and the even distribution of data points around the x-axis.

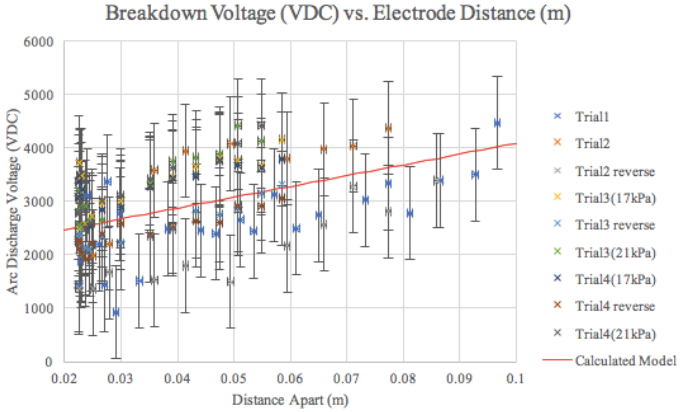

Fig. 11. Collected data with fitted model breakdown voltage (VDC) vs. electrode gap distance (m). Uncertainties calculated from SD.

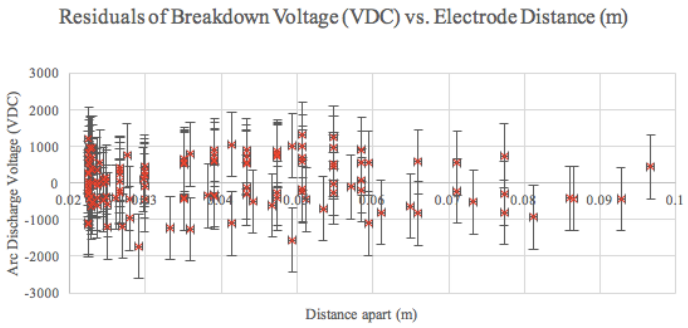

Fig. 12. Residuals plot for the electrical breakdown linear model.

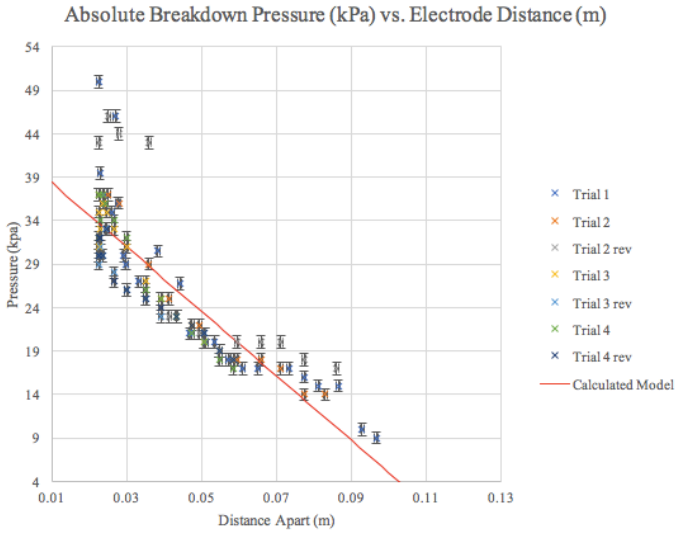

Fig. 13. Breakdown pressure (kPa) vs. electrode gap distance (m) data with plotted model. Uncertainties calculated from SD.

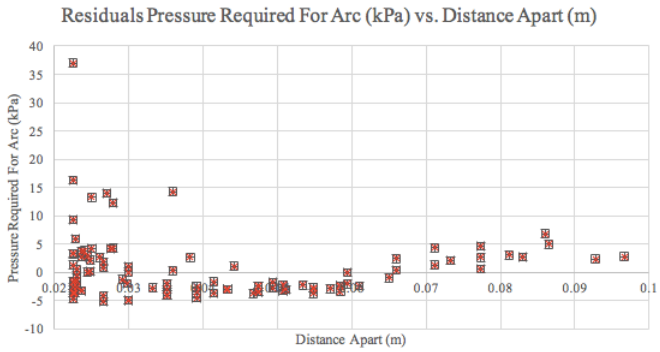

Figure 14. Residuals for the current model.

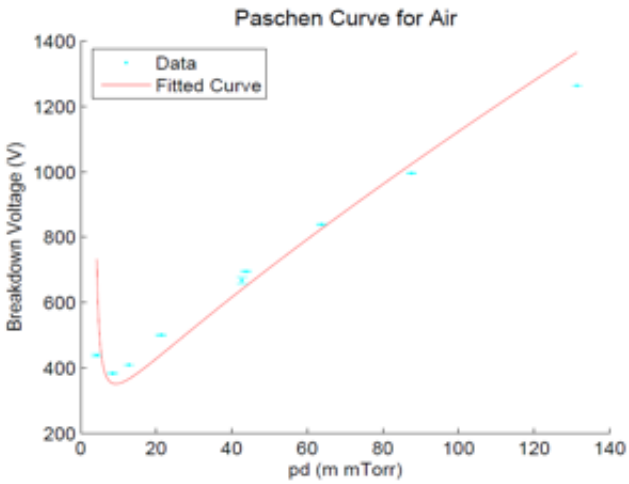

Figure 15. Experimental Paschen's curve for air. Taken without permission from Berzak et al., 2006.

Average Running Speeds of *Acheta domesticus* at Different Body Temperatures

Kelly (Xin) Wei
University of British Columbia, Vancouver, British Columbia, Canada

Abstract

The effects of different temperatures on Acheta domesticus speeds, based on metabolic changes, were determined to discover the biological implications on their survival during natural temperature fluctuations. As a result, the effects of both short term and long term climate change on the physical performance of house crickets can be assessed. Two separate treatment trials were conducted with hot and cold baths to attain three arenas of 20°C, 30°C and room temperature (22°C and 24°C). 10 replicates were placed into each arena and the average speeds of the crickets (cm/s) were found through tracing and timing. The crickets from Trial 1 had a larger mean speed difference and decreasing speeds with increasing temperatures, whereas the Trial 2 crickets had increasing speeds with increasing temperatures and a smaller difference in means. In both trials, the treatments resulted in sufficiently different speeds; however, the results were not statistically significant which indicates the null hypothesis, that states there is no difference between cricket speeds due to varying temperatures, cannot be rejected. Younger crickets in Trial 1 were more affected by temperature fluctuations and had speeds negatively correlated with temperature, whereas the older crickets in Trial 2 were less affected by temperature fluctuations but had speeds positively correlated with temperature. This suggests that younger crickets are less likely to survive in their natural habitats when temperatures slightly increase, while older crickets are more likely to survive when temperatures change; however, no definite conclusions can be made due to the experiment's statistical insignificance.

Introduction

Acheta domesticus, also commonly known as the house cricket, is native to arid areas of Northern Africa and southwestern Asia (Ghouri 1961). Due to the species' sentimental values and commercial purposes, the house crickets are intentionally distributed to other parts of Asia and Africa, as well as Europe and North America as pets and dietary supplements (Ghouri 1961; Walker 1999; Weissman et al. 2012). In North America, the crickets are commonly found in the eastern districts of the Great Plains, a grassland biome (Millburn n.d.). In their natural habitats, house crickets are located in slightly wet areas with tall weeds, such as logs, caves, and burrows, and generally emerge during the night, as they are nocturnal (Millburn n.d.). When exposed to cold weather, house crickets can also be found in buildings and homes due to their preference for the warm and humid environments provided by humans (Millburn n.d.).

House crickets' locomotion is primarily composed of crawling and jumping, both of which utilize knee extensions in their elongated hind legs (Hustert & Baldus 2010). In a study by Lailvaux, Hall & Brooks (2010), it was found that with greater locomotive abilities, which include jumping distance and power, the average lifespans of A. domesticus significantly increased; likewise, as jumping distances and power decreased, the average lifespans decreased as well. These results correspond to the results from a study by Hustert & Baldus (2010), who found that this ability to jump over large distances allowed A. domesticus to evade predators and defend themselves, helping maintain high survival. The crickets must also move quickly in order to catch their prey, suggesting that increased speeds again improve their fitness (Hustert & Baldus 2010). Additionally, the crickets' locomotion is also used to reproduce and avoid unfavorable environments with extreme temperatures (Lailvaux, Hall & Brooks 2010). As a result, there is a large positive

correlation between locomotive performance and lifespan, suggesting changes in the amount and rate of house crickets' movements directly influence their survival.

Due to the house crickets' ubiquitous distribution, the daily and seasonal temperature based on their natural location differs from place to place. However, field habitat temperatures fluctuate between 12.9°C to 20.3°C with a range from 10°C to 24°C daily; home habitat temperatures fluctuate between 20.9°C to 23.3°C with a range from 20.6°C to 24°C daily (Ciceran, Murray & Rowell 1993). Additionally, in the grassland biome of North America, winter temperatures can decrease to -17.8°C, while summer temperatures can reach 32.2°C (Bailey 2015). House crickets undergo metabolic changes during exposure to these temperature fluctuations; consequently, these shifts significantly affect A. domesticus' locomotive behavior, according to a study by Lachenicht et al. (2010). Lachenicht et al. (2010) also found that average running distances of A. domesticus rose with small to moderate rises in temperature, and that the average height of jumping also increased. However, as temperatures increased or decreased in large increments, both running speeds and jumping distances of the crickets decreased (Lachenicht et al. 2010). These results can be explained through the changes in the crickets' temperature-dependent metabolisms; both the A. domesticus' respiratory metabolisms, as well as standard metabolic rates, directly affect both the amount and speed of movements, according to Lachenicht et al. (2010). As the metabolic rates rise with small increases in temperature, the crickets are able to crawl more quickly and to jump larger distances (Lachenicht et al. 2010). The metabolic rates decrease, however, with large fluctuations in temperature, suggesting that maximal locomotion only occurs within a moderate, optimum temperature range (Lachenicht et al. 2010). If these temperature fluctuations influence the house crickets' ability to move efficiently, it would then also affect their survival; temperatures outside the optimum range would decrease the crickets' rate of movement, leaving them more susceptible to predators and less capable of capturing prey (Dangles et al. 2007).

In this experiment, we will measure the effects temperature fluctuation, within a relevant range, have on magnitude and speed of movement in the house cricket, A. domesticus. Generally, slight rises in temperature increase the standard metabolic rates of A. domesticus compared to decreases in temperature, allowing A. domesticus to travel greater distances at a faster speed, according to the results obtained from a study by Lachenicht et al. (2010). Therefore, we predict A. domesticus will crawl more, and more quickly, at slightly higher temperatures compared to lower temperatures due to these surges in metabolisms. The purpose of this study was to examine how slight-to-moderate temperature fluctuations, similar to those in global climate change and local home conditions, could affect the physical behavior of house crickets.

Methods

In this experiment, we measured the locomotive responses of Acheta domesticus to variations in temperature through the relative speeds (cm/s) of the crickets. Arenas with three temperatures were manipulated through two trials of separate treatments: the first consisted of two treatments of 30°C and a room temperature (control) of 24°C. The second trial consisted of three treatments: 20°C, 30°C, and 22°C (control).

Arena Set-up

Each treatment consisted of a sample size of 10 (n=10). The crickets were of small, medium, and large sizes, and were kept in constant extraneous conditions prior to and during experimentation: 316 lux light intensity (trial 1), 406 lux light intensity (trial 2), 200 mL of soil, 20s acclimation in the petri-dish, and 5s of acclimation in the arena before we began distance measurements. Some crickets moved a minimal amount due to not having limbs, indicating they were unhealthy. The unhealthy crickets were not used in the experiment to maintain consistency with trial results. We were unable to determine the crickets' sexes and we therefore chose randomly in order to minimize discrepancies in locomotive performance. Likewise, we were unable to determine the ages of the crickets, and thus chose randomly as well. We maintained the same numbers of different sizes in each treatment, to minimize response variations due to size.

Each cricket was only tested once.

Trials

In the first trial, we measured the speed responses with two treatments: room temperature (24°C) and 30°C. In the first treatment of 24°C, we did not manipulate the temperature, but just monitored it so that the temperature was maintained. The third treatment (30°C) consisted of a hot bath in which we heated water through a kettle and added it around the arena. It was covered by a plexi-glass cover to prevent floatation. The second trial included three treatments. The first treatment (20°C) consisted of an ice bath in which we placed ice in a bucket that surrounded the arena. The height of the bucket was again maintained through the experiment by using a plexi-glass cover to prevent the container from floating. The second room temperature (22°C) and third treatment (30°C) consisted of the same experimental set ups from trial 1. We maintained the temperatures by monitoring arena temperature with a thermometer between each replicate testing, and removing or adding ice or water.

We calculated the locomotive responses of the crickets by tracing over the plexi-glass, and measuring the distance the crickets moved, to determine the speed; in trial one, the distance was measured with a string and ruler, which would have resulted in a source of error due to the technical limits of human tracing. Our tracings were modified in trial two by using the image analysis software, JImage, in order to minimize time spent measuring and attain more accuracy. However, the source of error still remains, since the tracker relied on human tracing. We monitored the light intensity using a light intensity meter to reduce variation. In both trials, the same member traced crickets path to minimize the human uncertainty in measurements.

Statistical Analysis

We then inputted the data into Excel and online t-test calculators to determine the standard deviations, t-values, degrees of freedom, 95% confidence intervals, and p-values.

Results

In our first trial, the arena temperatures were 24°C and 30°C. The average speed for the 24°C treatment was 1.732cm/s (Fig. 1).

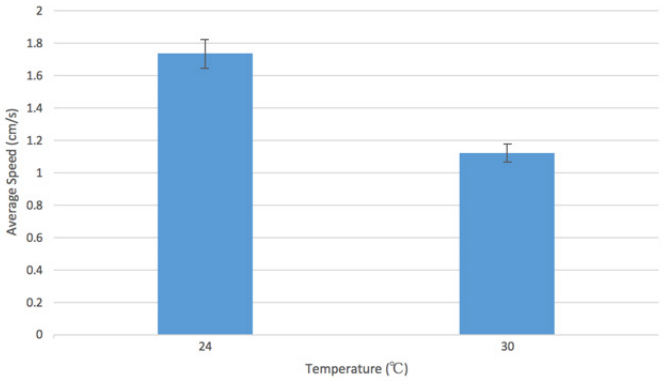

Figure 1. Trial 1 speed (cm/s) of house crickets, *Acheta domesticus*, when exposed to temperatures of 24°C (control) or 30°C. Bars represent the mean (± 95% confidence intervals) running speed in cm/s observed at 24°C (n=10) and 30°C (n=10).

The average speed for the 30°C treatment was 1.118cm/s. The 24°C treatment had a larger extreme value from the mean (3.50cm/s) while the 30°C treatment had a smaller extreme value (0.267cm/s). Based on Figure 1, there was a negative correlation between temperature and speed of movement. An increase in temperature was accompanied by a decrease in the speed of movement (y-axis). The p value is 0.113, which is larger than the alpha of 0.05; therefore, the difference between the means was not statistically significant and the null hypothesis could not be rejected. The t-value is 1.67; therefore, the two treatments resulted in sufficiently different speeds, but no concrete conclusions can be drawn. In both of our treatments, we observed that the crickets consistently ran in circular motions around the arena with some path retracing. In the 30°C treatment, more crickets tended to climb up walls.

In our second trials, the arena temperatures were 20°C, 22°C, and 30°C. The average speed for 20°C was 1.121cm/s (Fig. 2). The average speed for 22°C was 1.732 cm and the 30°C treatment had an average speed of 1.863cm/s. The standard deviation is 1.054. Based on Figure 2, there was a positive correlation between temperature and speed of movement. With an increase in temperature, we found there was an increase in the speed of movement. The p-value is 0.089, which is larger than the alpha of 0.05;

therefore, the difference between the means was not statistically significant and the null hypothesis could not be rejected. The t-value is 1.80; therefore, the two treatments resulted in sufficiently different speeds, but no concrete conclusions can be drawn. We observed that the crickets consistently ran around the arena in the same circular pattern with about half of them doubling back, retracing their path. The path retracing occurred more frequently in the control group (22°C) and occurred the least in the 30°C treatment, in which they moved forward the most.

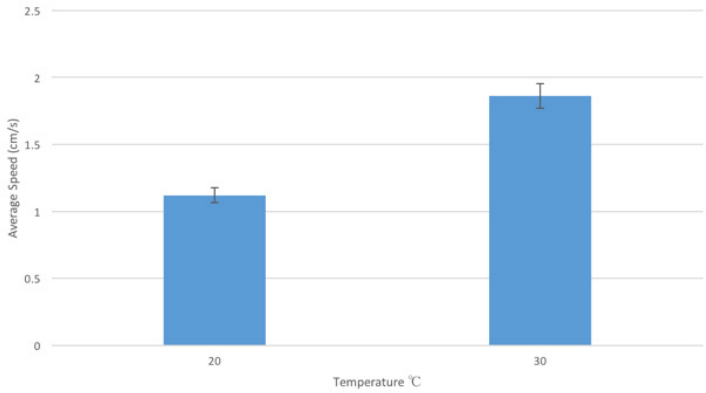

Figure 2. Speed (cm/s) of house crickets, *Acheta domesticus*, when exposed to temperatures of 20°C or 30°C. Bars represent the mean (± 95% confidence intervals) running speed in cm/s observed at 20°C (n=10) and 30°

Discussion

In this experiment, we found the effects on mean speeds of Acheta domesticus acclimated to three different body temperatures, in order to explore how temperature variations in natural habitats affect the crickets' survival rates. Although both of our trials were statistically insignificant, the overall trends in Trial 1 revealed younger crickets were more affected by variations in temperature and thus had a large difference in mean speeds, while the older crickets in Trials 2 were less affected by the same temperature changes, leading to a smaller difference in mean speeds. Both trials resulted in sufficiently different speeds; the Trial 1 crickets had speeds that decreased as temperatures were raised, while Trial 2 crickets had speeds that increased as temperatures increased.

In a study by Lachenicht et al. (2010), small increases in body temperature were shown to cause both standard metabolic and respiratory rates of house crickets to increase, allowing them to crawl and move faster relative to speeds at lower temperatures. We therefore predicted that the crickets would crawl/run more quickly at slightly higher temperatures than at lower temperatures due to these physiological effects. The results from Trial 1 were not consistent with our prediction; however, Trial 2 results were. In both cases, the results were not statistically significant.

The first study by Woodring, Roe, and Clifford (1977) examined the effects of age on metabolism in house crickets by measuring water and food consumption of 4800 female crickets at 30oC. They found that nymphs consumed high intakes of food in the beginning of each instar but decreased their intake during the latter portion of the instars. The nymphs continued this cycle until their final moult (8th instar), after which they became adults, and food and water intake began to level off; the results suggest that although younger crickets have higher metabolic rates compared to adults, their rates are also less stable and therefore more susceptible to abiotic factors (Woodring, Roe & Clifford 1977). The study by Woodring, Roe, and Clifford (1977) explains why smaller temperature fluctuations would have a larger impact on speeds of younger crickets by introducing metabolism based on age, which was not originally considered in our experiment. As a result, the discrepancy between the large difference in the younger crickets' mean speeds in Trial 1 compared to the older crickets' small difference in means in Trial 2, in our experiment, can be explained through the differing metabolisms between nymph and mature crickets.

Similarly to our experiment, the study by Lachenicht et al. (2010) also investigated the effects of body temperature variations on house crickets by testing the speeds of 400 randomly chosen adult crickets placed in arenas with temperatures ranging from 25 to 33oC (using water baths). Their study specifically examined the relationship between metabolism and temperature, which allowed them to determine that, although acclimation temperatures did not have an effect on speeds, average running speeds were generally higher with higher temperatures (Lachenicht et al. 2010). These results support our findings from Trial 2, where we found mean cricket speeds increased with temperature. However, the study's results contradict our findings from Trial 1, where mean speeds decreased with temperature elevations. This discrepancy may be due to the fact that adult crickets with stable metabolisms were used

both in the study by Lachenicht et al. (2010) and our Trial 2 treatments, but younger nymphs were used in our Trial 1 treatment; this age difference would affect the crickets' respective metabolic rates and consequently affect the mean speeds recorded in both trials.

The major source of variation in our experiment stems from the differing ages of the crickets used in Trial 1 and Trial 2. Trial 2 took place two weeks after Trial 1, therefore the crickets used in Trial 2 were older and more mature than the Trial 1 crickets. According to the study by Woodring, Roe, and Clifford (1977), the difference in the mean speeds of the crickets in Trial 1 and 2 was influenced by this age difference, as younger crickets have metabolic rates more vulnerable to abiotic changes; consequently, the adult crickets used in Trial 2 were less likely to be affected by abiotic temperature changes. Our data shows large temperature changes, and higher temperatures, cause mature crickets to have a smaller mean speed difference between the temperature treatments. Likewise, smaller temperature changes result in younger crickets having a large mean speed difference, which is supported by the age dependent metabolism results from the study by Woodring, Roe, and Clifford (1977). However, both trials resulted in no statistical significance.

Based on our results, older house crickets would be less affected by temperature changes but have increased speeds with elevated temperatures, while younger nymphs are more affected by temperature fluctuations and have decreased speeds with temperature increases in their natural habitats. These results can be explained through the differing metabolic rates between adults and nymphs, which suggest that survival rates and age are positively correlated (Roe, Clifford & Woodring 1980). In mature crickets, as temperatures rise and thus stable respiratory and standard metabolisms, they move more quickly, consequently enabling their ability to find food, such as sponges, and evade natural predators, such as centipedes (Hoefler, Durso & McIntyre 2012). Because of these temperature and age-dependent physiological changes, older crickets have improved chances of growing and reproducing with elevated temperatures, according to the results obtained from a study by Hustert and Baldus (2010). On the other hand, as temperatures increase by any amount, the speeds of younger crickets are negatively impacted due to their vulnerable metabolic rates; they would therefore be less likely to catch prey and additionally have an increased risk of predation, ultimately decreasing their fitness (Lailvaux, Hall & Brooks 2010).

The primary constraints in our experiment were the age differences between crickets used in Trial 1 and 2, as well as the gender ambiguity of the crickets chosen. The results were based on the effects of temperature on crickets; however, the crickets used in Trial 1 were much younger than those used in Trial 2, which affects our ability to generalize the results towards a population comprised of differently aged crickets. Since the genders and sex ratio of the crickets were unable to be specified, crickets were picked randomly; therefore our results cannot be applicable towards populations of drastically different sex ratios. In order to overcome these constraints, experimentation with large populations comprised of different age groups (more similar to those found in nature) would be necessary to observe the overall trends temperature have on cricket populations. In order to apply the results towards natural populations, the specific gender ratios of crickets in their natural habitat would also have to be established for future experiments, instead of focusing on segregated ages and random genders. The data can also be explained by the different temperature intervals for both trials. The room temperatures during each trial varied by 2°C, perhaps affecting the motion of the crickets. However, both resulted in similar average speeds, thus we would also need to consider the temperatures the crickets are acclimated to already, then test temperature changes relative to those.

In Trial 1, the general trend revealed that younger crickets had decreases in mean speeds when temperatures increased, refuting our hypothesis that higher temperatures will increase speeds due to the accompanying surges in metabolic rates. The Trial 1 crickets also had a larger difference in mean speeds compared to those in Trial 2, which may be due to their susceptible and unstable metabolisms. The trends in Trial 2 supported our hypothesis as the older crickets had speeds that increased when temperatures increased, and additionally had a smaller difference in mean speeds for each treatment; however, no definite conclusions can be gleaned from our experiment due to the statistical insignificance of both trials. A larger sample size would provide greater statistical robustness to this experiment.

References

Bailey, R 2015, Land Biomes: Temperate Grasslands. Available from: <http://biology.about.com/od/landbiomes/a/aa042106a.htm>. [4 February 2016].

Ciceran, M, Murray, A & Rowell, G 1994, 'Natural variation in the temporal patterning of calling song structure in the field cricket Gryllus pennsylvanicus: effects of temperature, age, mass, time of day, and nearest neighbour', Canadian Journal of Zoology, vol. 72, no. 1, pp. 38-42.

Dangles, O, Pierre, D, Christidès, JP & Casas, J 2007, 'Escape performance decreases during ontogeny in wild crickets', The Journal of Experimental Biology, vol. 210, no. 18, pp. 3165-3170.

Ghouri, ASK 1961, 'Home and Distribution of the House Cricket Acheta domesticus L', Nature, vol. 192, no. 4806, pp. 1000-1000.

Hustert, R & Baldus, M 2010, 'Ballistic movements of jumping legs implemented as variable components of cricket behaviour', The Journal of Experimental Biology, vol. 213, no. 23, pp. 4055-4064.

Lachenicht, MW, Clusella-Trullas, S, Boardman, L, Le Roux, C & Terblanche, JS 2010, 'Effects of acclimation temperature on thermal tolerance, locomotion performance and respiratory metabolism in Acheta domesticus L. (Orthoptera: Gryllidae)', Journal of Insect Physiology, vol. 56, no. 7, pp. 822–830.

Lailvaux, SP, Hall, M & Brooks, RC 2010, 'Performance is no proxy for genetic quality: Trade-offs between locomotion, attractiveness, and life history in crickets', Ecology, vol. 91, no. 5, pp. 1530-1537.

Millburn, N n.d., NATURAL HABITAT OF ACHETA DOMESTICUS. Available from: <http://animals.mom.me/natural-habitat-acheta-domesticus-1680.html>. [4 February 2016].

Walker, TJ 1999, 'House Cricket, Acheta domesticus (Linnaeus) (Insecta: Orthoptera: Gryllidae)', University of Florida IFAS extension. Available from: <https://edis.ifas.ufl.edu/pdffiles/IN/IN22000.pdf>. [4 February 2016].

Weissman, DB, Gray, DA, Pham, HT & Tijssen, P 2012, 'Billions and billions sold: pet-feeder crickets (Orthoptera: Gryllidae), commercial cricket farms, an epizootic densovirus, and government regulations make a potential disaster', Zootaxa, vol. 3504, no. 6, pp. 67–88.

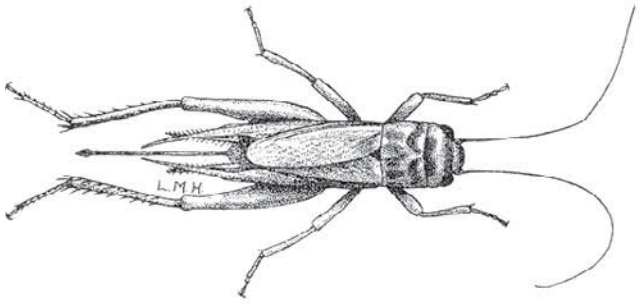

http://crawford.tardigrade.net/bugs/BugofMonth31.html

The Effectiveness of the Wilson Reading System on Multiple Measures of Literacy for a Braille-Reading Student with a Language-Based Learning Disability

Emily Van Gaasbeek
University of Toronto Mississauga, Mississauga, Ontario, Canada

Abstract

Visually driven and braille driven reading share common language attributes, yet the skills, cognitive load, and sensory system processing required to perform either task are dramatically different. Despite the significant differences in the processes of braille and print reading, traditional approaches to developing braille literacy have primarily relied upon adaptations of approaches used to establish sighted literacy. Furthermore, little research has investigated the effectiveness of these strategies for students who read braille. The outcomes, however, are clear; braille readers struggle to develop effective decoding and fluency skills. One promising literacy program, called the Wilson Reading System (WRS), has been adapted for braille literacy development because it emphasizes fluency and comprehension. Recent research suggests positive qualitative outcomes using the WRS for students with visual impairments. However, no quantitative changes in braille decoding and fluency using the WRS have been established. This case study extends previous findings to assess the effectiveness of the WRS on decoding ability, comprehension, oral fluency rate, and reading motivation in a braille-reading student with a language-based learning disability. Results demonstrate an increase in decoding ability, comprehension, reading motivation, but no sign of improvement in oral reading fluency.

Introduction

Print reading instruction involves five key hierarchical areas: phonemic awareness, phonics, fluency, vocabulary, and comprehension of text (National Reading Panel, 2000). In particular, reading fluency represents a combination of reading with speed, accuracy, and expression (Saviano & Hatton, 2013). Therrien and Kubina (2006) show that fluency is positively associated with a number of literacy outcomes to predict reading comprehension even better than direct measures of comprehension, such as questioning and re-telling. Visually impaired braille readers tend to experience difficulties developing reading comprehension and fluency (Savaiano, Compton, & Hatton, 2014), likely as a result of less incidental exposure to written language during early childhood, affecting the development of phonological awareness skills, decoding, and letter-sound recognition (Erickson & Hatton, 2007). Braille readers also lag behind in fluency compared to peers who are print readers because braille requires more cognitive resources as it utilizes tactile processing skills (Wright, Wormsley, & Kamei-Hannan, 2009). The tactile sensory system can only perceive objects one aspect at a time, compared with the visual sensory system that allows for simultaneous perception of objects. Thus, more cognitive resources are devoted to decoding braille, in a one-by-one manner, than print (Pring, 1994). In line with this theory, some research suggests braille readers devote more cognitive resources to word-level processes than print readers (Carreiras & Alvarez, 1999). There are additional challenges for visually impaired students in achieving reading fluency in the transition from reading

uncontracted, or alphabetic, braille, to contracted braille, which adds 189 contractions, or short-form words, to uncontracted braille (Herzberg, Stough, & Clark, 2004; Savaiano & Hatton, 2013).

Despite the significant differences in the processes of braille and print reading, reading intervention strategies for visually impaired students are adapted from strategies for sighted students. Many of these interventions have been shown to be unsuccessful for braille readers. For example, guided reading programs often utilize pictures to scaffold emerging vocabulary and comprehension. For students with visual impairments, this strategy is ineffective and fails to support learning (Kamei-Hannan & Ricci, 2015). The method for teaching phonics to sighted students is another example of an unsuccessful literacy strategy adapted for students with visual impairments. Sighted students first learn to recognize letters of the alphabet, and then use that knowledge to develop decoding skills. However, for students with visual impairments, research suggests teaching uncontracted, or alphabetic, braille alongside common contractions (e.g. "and," "but," "people") leads to improvements in vocabulary, decoding, and comprehension (Emerson, Holbrook, & D'Andrea, 2009; Kamei-Hannan & Ricci, 2015). Therefore, many of the literacy strategies used for sighted students are ineffective for use with students with visual impairments.

One promising intervention noted in qualitative research for improving literacy for students with visual impairments is the Wilson Reading System (WRS). The WRS is a twelve-step multisensory intensive reading program emphasizing direct instruction in phonics and phonological awareness that utilizes multisensory learning, such as visual, kinesthetic, auditory, and tactile methods of instruction (Ritchey & Goeke, 2006). Each highly structured lesson consists of ten sections that address all five components of reading recommended by the National Reading Panel - phonemic awareness, phonics, fluency, vocabulary, and comprehension of text (2000). The braille adaptation of the WRS is conceivably beneficial for students with visual impairments because it emphasizes fluency and comprehension, which are problematic areas for braille reading training (Savaiano, Compton, & Hatton, 2014). The braille version gradually introduces contractions within each stage of the system (Perkins School for the Blind, 2013), and progresses in difficulty only when automaticity is achieved in the current stage. The WRS takes around two to three years to significantly improve reading to match same-age peers.

For sighted students, quantitative research shows significant improvements in fluency, decoding, and comprehension after using the system (Duff, Stebbins, Stormont, Lembke, & Wilson, 2016; Stebbins, Stormont, Lembke, Wilson, & Clippard, 2012; Wilson & O'Connor, 1995;). In the adaptation of the WRS for the blind, some research has shown a qualitative benefit (Rowley, McCarthy, & Rines, 2014), but no quantitative evidence yet exists to reveal the full benefit of adapting the WRS for braille readers. The current case study will contribute to the emerging evidence of the WRS as an effective reading intervention strategy for students with visual impairments who are struggling braille readers. It is hypothesized that participants will experience an improvement in oral reading fluency rate, decoding, comprehension, and reading motivation following the intervention.

Methods

Participants

Participants were selected using the following criteria: participants 1) were identified as blind or low vision, and were receiving services through a Blind/Low Vision school program, 2) demonstrated average intelligence, 3) used braille as their primary literacy medium, 4) were identified as struggling braille readers according to teachers, and 5) were willing to participate in this study.

It is estimated that sixty-five percent of students with visual impairments also have multiple disabilities (Ivy & Hatton, 2014). Many of the possible participants for this study were disqualified because they had multiple disabilities, including intellectual disabilities. Further, only one student consented to participation in this study. Thus, only one participant fit the criteria for this study. The participant was enrolled in Grade 8, was receiving services from the Blind/Low Vision program in his school district, and used braille as his primary literacy medium. According to the participant's individual education plan, he has been diagnosed with a language-based learning disability, is of average intelligence, and reads at a Grade 6 level.

Experimental Design

A case study design was utilized in this study to examine the effectiveness of the WRS for improving oral reading fluency, comprehension, decoding ability, and reading motivation. The case study design is commonly used in educational research, often in program evaluation (Crossley & Vulliamy, 1984). With a case study design, curriculum can be investigated deeply, focusing not only on the final learning outcome but also on the processes of learning itself (Crossley & Vulliamy, 1984). Furthermore, visual impairment is a low-incidence disability; thus a case study was suitable given the small population size (Hatton, 2014).

Materials

The WRS, including a Level 2B Student Reader, Level 2B supplemental braille worksheets, magnetic print-braille letter tiles, sound cards, and word cards, was used for the baseline measurements and the intervention (Wilson, 2013a; Wilson 2013b). Level 2B was chosen instead of Level 1B, 1A, or 2A due to the participant's age and grade level (Wilson, 2013a). The Wilson Assessment for Decoding and Encoding (WADE) was used for baseline and intervention measurements of decoding ability, and the Motivation to Read Profile – Revised was used for pre- and post-intervention measurements of reading motivation (Malloy, Marinak, Gambrell, & Mazzoni, 2013; Wilson, 1998). The sound cards, word cards, and magnetic braille tiles of the WRS were in uncontracted Unified English Braille (UEB), while the supplemental braille worksheets were in contracted UEB. The WADE was in uncontracted UEB. The Motivation to Read Profile – Revised was delivered orally (Malloy, Marinak, Gambrell, & Mazzoni, 2013). Comprehension was assessed using an uncontracted braille copy of a grade-appropriate novel, I am a Taxi, that the student was reading and discussing in his class at school (Ellis, 2006). Two different passages were used for the baseline measurement and the post-intervention measurement. Additionally, a stopwatch was used to collect data on oral fluency rate.

Measurements

There were four dependent variables measured within this case study: 1) oral fluency rate, 2) decoding ability, 3) comprehension, and 4) reading motivation. These variables were chosen because they are consistently measured in literacy studies, particularly in studies on the effectiveness of the WRS (Duff, Stebbins, Stormont, Lembke, & Wilson, 2016; Stebbins, Stormont, Lembke, Wilson, & Clippard, 2012; Wilson & O'Connor, 1995).

Oral reading fluency was represented as the number of read words per minute (wpm). Experienced braille readers tend to read around 70-100 wpm (Pring, 1994). The participant read two different uncontracted braille passages from I am a Taxi, an age-appropriate novel he was reading and discussing at school, one passage during the baseline phase, and a different passage after the intervention period (Ellis, 2006).

Decoding ability was measured using the WADE (Wilson, 1998). The WADE is made up of three sections: 1) sounds, 2) reading, and 3) spelling. In the sounds section, the participant was asked to identify the sound of various graphemes, including consonants, digraphs and trigraphs, vowels, and welded sounds. In the reading section, the participant was asked to read from three progressively challenging lists of real words and nonsense words – words that did not follow the rules of the English language. In the spelling section, the participant was asked to orally spell words and the percentage correct score was reported.

Comprehension was defined in this study as the percentage of content words provided by the participant in an oral retelling following the participant reading a passage from I am a Taxi (Ellis, 2006). Content words were nouns, adjectives, or verbs chosen by the researcher for their relevance to the understanding of the passage (Savaiano & Hatton, 2013). The oral retelling consisted of the participant telling the researcher about the preceding passage in as much detail as possible.

Reading motivation was orally assessed using the Motivation to Read Profile – Revised, which consisted of twenty questions regarding the participant's value and self-concept as a reader. The value and self-concept scores were both scored out of a maximum of 40 points. The two scores together represented the reading motivation score, out of a possible 80 points (Malloy, Marinak, Gambrell, & Mazzoni, 2013). The participant declined to answer one question in the Motivation to Read Profile – Revised; therefore, the reading motivation score in this case study was out of a possible 76 points.

Procedure

In the baseline phase, data were collected on oral fluency rate and comprehension. The participant read passages from I am a Taxi for the collection of these data (Ellis, 2006). The participant would read three to five passages that were timed by the researcher and was asked to retell the passage using great detail. The baseline phase consisted of three sessions, approximately thirty minutes each.

Intervention

In the intervention phase, the participant was guided through Level 2B of the WRS (Wilson 2013a). The session would begin with a sound cards drill using the Wilson Level 2B sound cards, focusing on phonemic awareness and phonics. These cards would be in both uncontracted and contracted UEB. Then the participant would read aloud the Wilson Level 2B word cards to improve automaticity and fluency, in uncontracted and contracted braille. The participant would then read a list of contracted words from the Wilson Level 2B supplemental braille worksheets. After reading the words, the participant would read sentences from the Wilson Level 2B Student Reader in contracted braille. Finally, the participant would read a passage in contracted braille from the Wilson Level 2B Student Reader, and then would answer comprehension questions regarding the passage from the Wilson Level 2B supplemental braille worksheets. Each lesson took approximately one hour to complete. The data were collected over eight sessions, and was constrained to the academic year. Following the last lesson in the intervention phase, data were collected to measure changes in oral reading fluency, decoding, comprehension, and reading motivation.

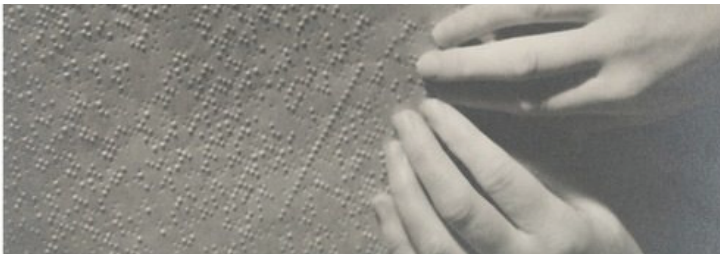

Results

Decoding Ability

Decoding ability is a measure of letter-sound recognition (Erickson & Hatton, 2007), and results are presented in Table 1. In the sounds portion of the WADE, there was an increase in the percentage correct score for consonants and vowel sounds, while there was no change in digraphs/trigraphs or welded sounds. In the reading portion of the WADE, there was an increase in the percentage correct score for Reading List 2 and Reading List 3, while there was no change in Reading List 1. In the spelling portion of the WADE, there was no change in the percentage correct score from the baseline to after the intervention. Overall, the participant experienced an increase of 3.5% in decoding ability.

Table 1. Results of the Wilson Assessment of Decoding and Encoding

	Baseline (percent correct)	Post-intervention (percent correct)	Percent Change
Consonants	91.6	95.8	4.2
Digraphs/Trigraphs	83.3	83.3	0
Vowel sounds	83.3	100.0	16.7
Welded sounds	100.0	100.0	0
Reading List 1	100.0	100.0	0
Reading List 2	93.3	100.0	6.7
Reading List 3	80.0	93.3	13.3
Spelling	81.8	81.8	0

Comprehension

During the baseline phase, the participant retold an average of 58.6% (range 41% - 75%) of content words. Following the intervention, the participant retold an average of 72.7% (range 67% - 80%) of content words, for an increase of 14.1%.

Reading Motivation

During the baseline phase, the participant scored 62 out of 76 on the Motivation to Read Profile – Revised (Malloy, Marinak, Gambrell, & Mazzoni, 2013). Following the intervention, the participant scored 71 out of 76, for an increase of 11.8%.

Oral Fluency Rate

Oral reading fluency was represented as the number of read words per minute (wpm). The participant had a baseline oral fluency rate of 61 wpm in uncontracted braille reading after three sessions. Following the intervention, the participant had an oral fluency rate of 47 wpm in uncontracted braille reading, for a decrease of 22.9%.

One unexpected improvement not previously identified within the experiment was the participant's improvement in contracted braille. Prior to the intervention, the participant knew a few braille contractions, but through the intervention, the participant experienced a qualitative improvement in his knowledge of contractions.

Discussion

The results of this study indicate that the WRS may be effective for struggling braille readers in improving comprehension, decoding ability, and reading motivation. The participant experienced a 14.1% increase in comprehension, an overall increase of 3.5% in decoding ability, and an 11.8% increase in reading motivation following the eight sessions. These results demonstrate that the WRS, adapted to visually impaired readers, does indeed quantitatively benefit improvement in areas of literacy where braille-reading students lag behind sighted peers (Erickson & Hatton, 2007; Savaiano, Hatton, & Compton, 2014).

Results revealed no sign of improvement, and in fact, a slight decrease, in oral reading fluency after the intervention. It is important to note that the participant was concurrently receiving uncontracted braille training at school during the course of the intervention. Although the participant's oral reading fluency did not improve, a more salient result of this study was the participant's increased understanding of contractions. While there is no quantitative evidence to support this claim, the participant frequently noted that he perceived a greater fluency in his ability to read contractions as a result of the intervention. Since fluency was measured using uncontracted braille passages, contracted braille fluency was not accurately measured to quantify this improvement. Additionally, qualitative measures of the WRS for braille-reading students revealed improvements in fluency over longer periods of time, such as two years, suggesting similar quantitative results could be achieved in an extended time frame (Rowley, McCarthy, & Rines, 2014). Furthermore, despite the decrease in oral reading fluency, the participant did experience an increase in three out of the four measures.

Limitations

Although the case study design is useful in investigating instructional strategies more in-depth than larger quantitative studies, the research is limited in its generalizability (Crossley & Vulliamy, 1984). Furthermore, the population of braille readers is small and heterogeneous, so the WRS may vary in its effectiveness for students with other needs or disabilities (Hatton, 2014). The only other case study conducted on the use of the WRS for braille readers had two participants, so although the research base is small, this study has contributed to its growth (Rowley, McCarthy, & Rines, 2014).

The positive results in comprehension in this case study may also be limited. The improvement in comprehension may have been influenced by classroom instruction the participant was receiving regarding I am a Taxi, in the form of discussions of the novel's themes. Although the comprehension assessments in the intervention asked the participant to recall specific details, not necessarily overall themes, from a two- to three-minute passage read by the participant, it is still plausible that outside instruction could have affected the results.

Another major limitation was the time constraint of this study. As this research was confined to an academic year, the WRS could not be completed in its entirety. Since the WRS takes two to three years to complete, a longer time frame would have increased the study's validity (Wilson & O'Connor, 1995). The WRS has demonstrated to be effective for sighted students when examined for one to two years, and qualitative results using braille-reading students yielded similar results (Duff, Stebbins, Stormont, Lembke, & Wilson, 2016; Rowley, McCarthy, & Rines, 2014; Stebbins, Stormont, Lembke, Wilson, & Clippard, 2012; Wilson & O'Connor, 1995). Even over a short period of time, the improvements in comprehension, decoding ability, and reading motivation in this study reveal the positive impact of the adapted WRS for the visually impaired.

Implications for Future Research

The results of this study suggest the WRS is an effective practice for use with braille-reading students with language-based learning disabilities. The WRS has been quantitatively demonstrated to be an effective strategy for improving fluency, decoding, and comprehension (Duff, Stebbins, Stormont, Lembke, & Wilson, 2016; Stebbins, Stormont, Lembke, Wilson, & Clippard, 2012; Wilson & O'Connor, 1995). Fluency, comprehension, and decoding are key measures of literacy for both print and braille readers (Savaiano & Hatton, 2013). Qualitative evidence has shown that the WRS may be effective in improving comprehension, decoding ability, and oral reading fluency for struggling braille readers (Rowley, McCarthy, & Rines, 2014). The current case study enhances these findings by adding

quantitative measurements of comprehension, decoding ability, oral reading fluency, and an added component of reading motivation, which is a key predictor of overall literacy achievement (National Reading Panel, 2000). An unexpected result of the current case study was the effect of the WRS on qualitatively improving contracted braille reading fluency. Further research should be conducted using a larger sample, over a longer period of time, to accurately measure the effectiveness of the system on a more diverse sample of braille readers. If the current research were to be replicated, greater quantitative focus should be paid to the effectiveness of the WRS in oral reading fluency for contracted braille. Such a focus would have implications for using the WRS for struggling, beginning braille readers.

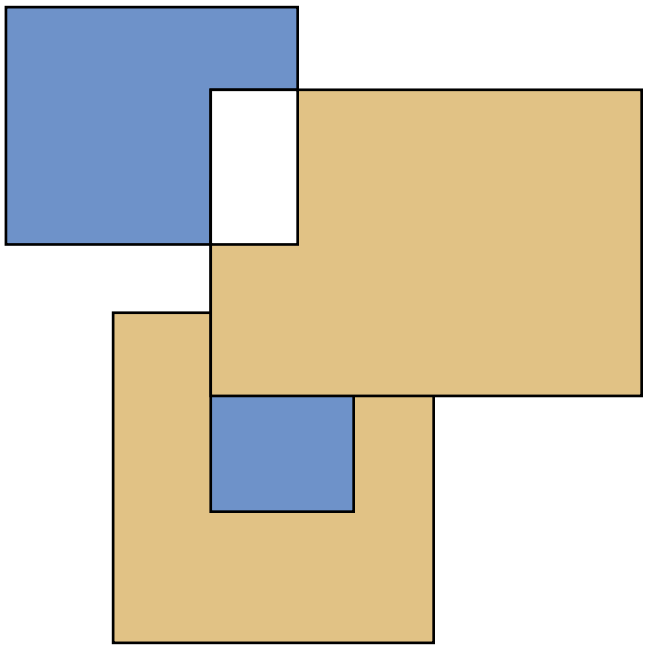

References

Carreiras, M., & Alvarez, C. J. (1999). Comprehension Processes in Braille Reading. Journal of Visual Impairment & Blindness, 93(9), 589-595. Retrieved from https://eric.ed.gov/?id=EJ594920

Duff, D., Stebbins, M. S., Stormont, M., Lembke, E. S., & Wilson, D. J. (2016). Using curriculum-based measurement data to monitor the effectiveness of the Wilson Reading System for students with disabilities: an exploratory study. International Journal on Disability and Human Development, 15(1), 93-100. doi:10.1515/ijdhd-2015-0007

Ellis, D. (2006). I Am a Taxi. Toronto, ON: Groundwood Books Ltd.

Emerson, R. W., Holbrook, M. C., & D'Andrea, F. M. (2009). Acquisition of literacy skills by young children who are blind: Results from the ABC Braille Study. Journal of Visual Impairment & Blindness, 103(10), 610-624. Retrieved from https://www.researchgate.net/profile/Robert_Wall_Emerson/publication/286232902_Acquisition_of_Literacy_Skills_by_Young_Children_Who_Are_Blind_Results_from_the_ABC_Braille_Study/links/570fe16908aefb6cadaaa18d.pdf

Emerson, R. W., Sitar, D., Erin, J. N., Wormsley, D. P., & Herlich, S. L. (2009). The effect of consistent structured reading instruction on high and low literacy achievement in young children who are blind. Journal of Visual Impairment and Blindness, 103(10), 595-609. Retrieved from http://www.afb.org/jvib/jvibabstractNew.asp?articleid=jvib031004

Erickson, K. A., & Hatton, D. (2007). Literacy and visual impairment. Seminars in Speech and Language, 28(1), 58-68. doi:10.1055/s-2007-967930

Erin, J., & Hong, S. (2004). The impact of early exposure to uncontracted braille reading on students with visual impairments. Journal of Visual Impairment & Blindness, 98(6), 325-340. Retrieved from http://files.eric.ed.gov/fulltext/EJ683608.pdf

Fuchs, L. S., Fuchs, D., Hosp, M. K., & Jenkins, J. R. (2001). Oral reading fluency as an indicator of reading competence: A theoretical, empirical, and historical analysis. Scientific Studies of Reading, 5(3), 239-256. doi:10.1207/S1532799XSSR0503_3

Hatton, D. D. (2014). Advancing the Education of Students with Visual Impairments Through Evidence-Based Practices. Current Issues in the Education of Students with Visual Impairments, 46, 1-22. doi:10.1016/B978-0-12-420039-5.00001-0

Herzberg, T. S., Stough, L. M., & Clark, C. M. (2004). Teaching and Assessing the Appropriateness of Uncontracted Braille. Research Report. Journal of Visual Impairment and Blindness, 98(12), 773-779. Retrieved from http://files.eric.ed.gov/fulltext/EJ683784.pdf

Kamei-Hannan, C., & Ricci, L. A. (2015). Reading Connections: Strategies for Teaching Students with Visual Impairments. New York, NY: American Foundation for the Blind Press.

Malloy, J. A., Marinak, B. A., Gambrell, L. B., & Mazzoni, S. A. (2013). Assessing motivation to read. The Reading Teacher, 67(4), 273-282. doi:10.1002/trtr.1215

National Reading Panel (US), National Institute of Child Health, & Human Development (US). (2000). Teaching children to read: An evidence-based assessment of the scientific research literature on reading and its implications for reading instruction. Retrieved from https://www.nichd.nih.gov/publications/pubs/nrp/documents/report.pdf

Perkins School for the Blind. (2013). Wilson Reading System: Adapted for Students who are Blind and Visually Impaired. Louisville, KY: American Printing House

Pring, L. (1994). Touch and go: learning to read Braille. Reading Research Quarterly, 67-74. doi:10.2307/747738

Ritchey, K. D., & Goeke, J. L. (2006). Orton-Gillingham and Orton-Gillingham—based reading instruction a review of the literature. The Journal of Special Education, 40(3), 171-183. doi:10.1177/00224669060400030501

Rowley, R., McCarthy, M., & Rines, J. C. (2014). Adaptation of the Wilson reading system for braille readers. Journal of Visual Impairment & Blindness, 108(2), 146-150. Retrieved from http://connection.ebscohost.com/c/articles/97076576/adaptation-wilson-reading-system-braille-readers

Savaiano, M. E., & Hatton, D. D. (2013). Using repeated reading to improve reading speed and comprehension in students with visual impairments. Journal of Visual Impairment and Blindness, 107(2), 93-106. Retrieved from http://www.afb.org/jvib/jvibabstractNew.asp?articleid=jvib070203

Savaiano, M. E., Compton, D. L., & Hatton, D. D. (2014). Reading comprehension for braille readers: An empirical framework for research. International Review of Research in Developmental Disabilities, 46, 177-206. doi:10.1016/B978-0-12-420039-5.00004-6

Stebbins, M. S., Stormont, M., Lembke, E. S., Wilson, D. J., & Clippard, D. (2012). Monitoring the Effectiveness of the Wilson Reading System for Students with Disabilities: One District's Example. Exceptionality, 20(1), 58-70. doi:10.1080/09362835.2012.640908

Steinman, B. A., LeJeune, B. J., & Kimbrough, B. T. (2006). Developmental stages of reading processes in children who are blind and sighted. Journal of Visual Impairment & Blindness, 100(1), 36-46. Retrieved from http://files.eric.ed.gov/fulltext/EJ726264.pdf

Therrien, W. J., & Kubina, R. M. (2006). Developing reading fluency with repeated reading. Intervention in School and Clinic, 41(3), 156-160. doi:10.1177/10534512060410030501

Wilson, B. A., & O'Connor, J. R. (1995). Effectiveness of the Wilson Reading System used in public school training. Clinical studies of multisensory structured language education, 247-254. Retrieved from http://www.wilson-language.com/wp-content/uploads/2015/04/Evidence_OConnor_Wilson.pdf

Wilson, B. A. (1996). Wilson Reading System: Instructor Manual. Oxford, MA: Wilson Language Training Corporation.

Wilson, B. A. (1998). Wilson WADE user's guide: Wilson assessment of decoding and encoding. Oxford, MA: Wilson Language Training Corporation.

Wilson, B. A. (2013a). Wilson Reading System: Student Reader 2. Louisville, KY: American Printing House for the Blind, Inc.

Wilson, B. A. (2013b). Wilson Reading System: Supplemental Braille Worksheets 2. Louisville, KY: American Printing House for the Blind, Inc.

Wright, T., Wormsley, D. P., & Kamei-Hannan, C. (2009). Hand movements and braille reading efficiency: data from the Alphabetic braille and Contracted braille Study. Journal of Visual Impairment and Blindness, 103(10), 649-662. Retrieved from http://www.afb.org/jvib/jvibabstractNew.asp?articleid=jvib031008

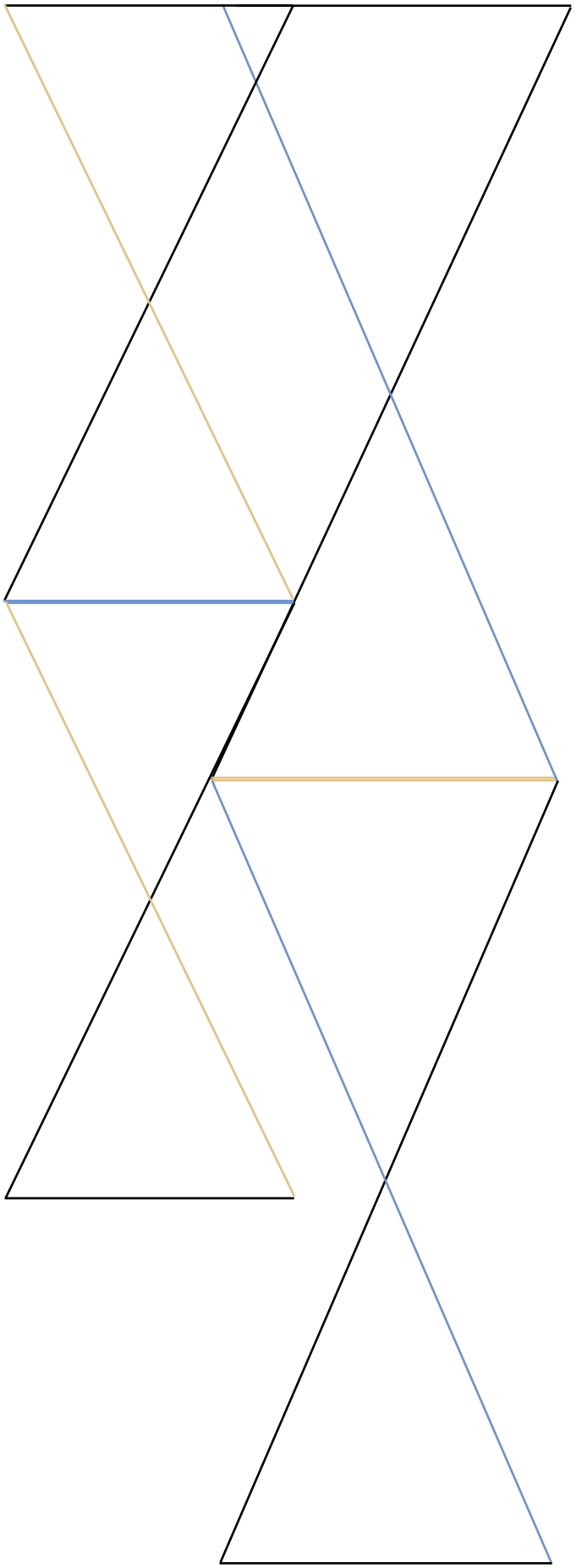

Can We Be Proud Of Pride? A Discussion on Intersectionality in Current Canadian Pride Events

Grace Berit Marshall
Vancouver Island University, Nanaimo, British Columbia, Canada

Introduction

Pride emerged as a radical demonstration of the lesbian, gay, bisexual, transgender, and queer (LGBTQ) civil rights movement. Over the years, its purpose and form have evolved. While Pride is a necessary source of LGBTQ representation, it often fails to observe the intersectionality within its community, resulting in racism, ableism, sexism, homophobia, classism, and homonormativity. This essay explores this lack of intersectionality, drawing on Nanaimo Pride as a source of discussion, with references to celebrations in Edmonton, Toronto, and New York. It concludes by offering suggestions for making Pride more inclusive.

Background

The LGBTQ civil rights movement in North America is largely attributed to the Stonewall riots, which were protestations of police surveillance and criminalization of LGBTQ bodies. Gay civil rights movements, groups, and demonstrations increased in frequency throughout North America after the Stonewall riots of 1969, and in 1972, Canada held its first Pride celebration in Toronto. This was not representative of a more tolerant general population, but rather a more vocal LGBTQ community (Rau). The LGBTQ community continued to face legalized discrimination and persecution into the early 2000s. Police raids of lesbian and gay bathhouses were common, with the last major raid taking place in Toronto, 2000 (Rau). It took until July 20th, 2004, for same-gender marriage to be legalized across Canada. It is important to note here that these social changes are not trailblazing initiatives, but rather echos of previous equity on this landscape—before the colonization of Canada, cis- and heteronormative policing was not the norm. For instance, many Indigenous Nations celebrated individuals with two-spirit identities, which have been described as Indigenous people "born with masculine and feminine spirits in one body" (Sheppard 262). Indigenous Nations had many ways of conceptualizing gender and sexuality that were different from European cultures (Sheppard 262).

In 2016, the first formal Pride parade in Nanaimo, British Columbia, was held. Thousands of people showed up to observe the parade, and dozens of floats and walking groups participated. This was a major surprise to those of us participating in the parade, as Nanaimo does not have a history of being a queer-friendly city. The current Nanaimo Pride Society President, a Nanaimo-local gay man, says he moved away from Nanaimo in his youth because of the repressive atmosphere (Stern). This is something a lot of LGBTQ people who lived in Nanaimo in the 80s, 90s, and early 2000s have said: not only were they likely to get assaulted outside of Spike, the only gay bar in town, but the city council often had very bigoted people in very respected positions. An example of this was that "in 2000, half of Nanaimo City Council walked out of a council meeting after being asked to sign a Gay Pride Day Proclamation," including the then-mayor Gary Korpan (Stern). The Pride Day Proclamation was consistently shut down, until the major pride association of the time threatened Korpan with a human rights complaint (Christopher).

Given this history, the 2016 Nanaimo Pride parade meant an immense amount to many people. It didn't spring up from the ground, but was the direct result of the hardworking members of the community who fought for years to make this event happen. Pride represented not only a moving on from a

bigoted past, but also solidarity in the face of tragedy. Early that morning, on June 12th, the largest mass shooting in American history occurred at a gay bar in Orlando, Florida, with 49 people killed and 53 people injured. The Pulse nightclub shooting was and continues to be the largest mass shooting in American history, being so bloody that "[o]ne out of every three people in the club [were] wounded or killed" (Santora). This horrific hate crime sent ripples throughout the LGBTQ community, and its effects were felt acutely as Pride month went on. In Nanaimo, the Pride flag flew at half-mast. I would, then, describe the 2016 Nanaimo Pride parade as nothing less then necessary.

Intersectionality

To understand this paper, one must have an understanding of intersectionality. Intersectionality, as defined in Kimberle Crenshaw's formative essay on the topic, "Traffic at the Crossroads: Multiple Oppressions," is the "interactive effects of discrimination" (43). This is visualized in her essay as a traffic intersection, wherein the roads represent the institutions of power in the world, and people with power held over them are trying to navigate the intersection. Crenshaw specifically wrote this paper to illuminate the experiences of black women, and the ways in which their gender and race interacted. The intersections with more roads are busier and more complicated, making them more dangerous to navigate. Crenshaw extends this metaphor to illustrate that the cars moving through the intersection represent the daily, seemingly mindless, actions that reify these power imbalances. Finally, ambulances called to these busy intersections have a difficult time getting there, and may in fact be too late to help. A crash or accident, in this case, would refer to the person navigating the intersection becoming harmed in some way. This could be a singular, spectacular incidence—a physical assault, or an eviction—or it could be a subtle erosion of autonomy, mental health, or self-worth. These micro and macro aggressions create a complex situation for people suffering from layered oppressions, posing a challenge for the figurative ambulances.

To give an example of intersectionality, there could be a homeless young woman, who is also lesbian and First Nations. She would be experiencing discrimination from multiple fronts: those of her gender, her race, and her sexuality. Her age would place her at a disadvantage, as she wouldn't have the full independence of an adult. She might experience outreach from programs centred on homeless LGBTQ youth, but they might not recognize the effect of the colonization of First Nations people that could play into her situation. The same thing could be said if she gained asylum at a women's shelter; they could understand why she, as a young woman, might be in a precarious situation, but not be able to understand how her lesbianism affects her situation. In this way, these "ambulances" are rendered less effective to those who experience multiple marginalized social categories. In general, "it is difficult to talk about how one of [...] many identifiers may contribute to one phenomenon," as "[i]dentities are interlocking" (Pastrana 101). In the hypothetical situation above, the intervention methods are failing because they are treating this person's identities as "separate experiences rather than a complex and dynamic relationship" in which teasing apart the influences of each can be difficult or impossible (Fox 633).

Pride is an ambulance, as it resulted from the need of a marginalized community to be seen and heard for one day a year, if nothing else. The Stonewall riots resulted directly from the fact that an intersectional LGBTQ community had been pushed to the boiling point, by criminalization and discrimination from every angle (Born). These riots helped the LGBTQ communities to gain momentum to push for further demonstrations (Born). When a legal or policy shift occurs, such as the decriminalization of sex between gay men, the acceptance of gay men and women into the military, the option for same-gender couples to adopt children, or the legalization of same-gender marriage, it is not the master choosing to throw a bone to a well-behaved dog. The bone must be taken whether the master wants it or not. It is only through the unwanted, yet continual, vocal push from marginalized communities that such changes are made. This is evident in my home community of Nanaimo, where the local government had to be petitioned and argued with—sometimes even threatened with legal action—for several years before a Pride day could be officially recognized. Change is not easily won. Pride, then, should be an event to recognize and celebrate the diversity within its community, and to acknowledge the members that are most vulnerable.

Homonormativity

Pride parades and events in their current forms fail to do this. While Pride started out as a series of riots and demonstrations, in urban areas, it is now a government- and corporate-funded, highly attended event. By accepting this sponsorship, Pride has become an institution, and has fallen prey to replicating the systems of power it is meant to expose and oppose. It is, "[i]ronically, our efforts to challenge one form of oppression [that] often unintentionally contribute to other forms of oppression, and our efforts to embrace one form of difference exclude and silence others" (Fox 631). One way Pride does this is in celebrating "the ideal queer person." This person can be found centred on Pride parade posters, as the MC of events, and on any advertising for year-round functions. This hypothetical person is a white, able-bodied, upper-middle class, cisgender, neurotypical, and young gay man. There is a reason this description has become the poster for Pride, and it is because it appeals to straight mentality. A person like this is similar enough to a straight person that they can forget the "otherness" of queerness. They can comfortably watch shows that have this person as the token, tropic gay character, and they don't have any problem with this gay man coming to their barbecue. In this way, they can be an "ally" without ever having to engage with the harsh realities of queer existence, or the idea that queer people might actually be different than them. Pride tends to indulge this idea, placing straight people's sensibilities above the actual needs of LGBTQ people. When "[w]hite gay male sexualities and desires are privileged and normalized," a concept known as homonormativity emerges (Greensmith 133). Homonormativity "upholds and sustains [heteronormativity] while promising the possibility of a demobilized gay constituency and privatized, depoliticized gay culture anchored in domesticity and consumption" for non-LGBTQ audiences (Greensmith 133). This homogenization of queer culture is one of the ways in which a faulty institution of Pride is created.

Racism

In addition to the solidification of homonormativity, Pride contradicts its own purpose of inclusivity through the mistreatment of racial minorities within the community. One way this manifests is in the presence of police at Pride. Queer people have a fraught history with the institution of police—one that continues today. The relationship of racial minorities with police is similarly, if not more, fraught. In "How a Black Lives Matter Toronto Co-Founder Sees Canada," Janaya Khan says of her first day at Pride: "Having been [at Pride] for about 20 minutes I had my very first interaction with police at Pride. I have a history with interaction with police that hasn't gone very well for me" (Khan). As a black person who identifies as "queer and as gender non-conforming," Khan's encounters with police were "very aggressive," with the officer "demanding ID and wanting information about where [they were] going" (Khan). So, police have a history of being violent and discriminatory against queer people, and the same thing against people of colour (POC). As the Black Lives Matter (BLM) movement shows us, we are also currently experiencing an epidemic of police brutality against black people (Wortley 53). What does it say of Pride's priorities that police have their own honoured place among the festivities, often getting their own float? It speaks both to white supremacy and to an erasure of history. There are lovely police officers, and there are queer police officers. But there is no need to attend Pride in uniform, placing oneself in a position of power over the others attending. Read generously, this is an attempt to mend the relationship between the LGBTQ community and the police force. In actuality, having police at Pride does more harm then good to the POC in attendance.

Not everyone agrees that police should not march in Pride parades, however. A news article covering the same issue of BLM Toronto staging a peaceful sit-in at the Toronto Pride parade—the subject of Khan's aforementioned interview—says that "[a]fter being given honorary status, it was shameful of Black Lives Matters to disrupt the parade and for Pride for agreeing to its terms" (Jamieson). The author goes on to say that "[he is] proud to be a gay black man in Canada," and that he believes that "BLM has absolutely nothing to do with the gay, lesbian, transgendered community" (Jamieson). This is a viewpoint lacking an intersectional lens. Black people are part of the LGBTQ community; the author himself is a black, gay man. If members of the LGBTQ community are facing extreme police brutality, for whatever reason, it should be a concern for the community at large. In a study focusing on the intersectionality of POC and their queer

identities, two separate participants admitted that their identities alienated them from both the LGBTQ community and their racial communities. One participant says that: "Working within my racial community is a hindrance, as a LGBTQ-identified person [...] there is no support there," while another says, "[s]ometimes, in the [gay, lesbian, bisexual, and transgender] GLBT community, I feel being Black may work against me because there is so much racism" (Pastrana 99). Clearly, there is a need for more acceptance of intersectionality between the LGBTQ and racial minority communities.

Aside from lacking an intersectional analysis, Jamieson, the author of the critical news piece, also argues that Pride has been apolitical regarding non-LGBTQ issues, stating that "[h]istorically, Pride has distanced itself from political issues not pertaining to members of the LGBTQ community" (Jamieson). In this regard, Jamieson's assertion is incorrect. Firstly, if someone is queer, then that makes the other aspects of their identity important to LGBTQ activism. To assert the opposite seems unnecessarily divisive. Secondly, some of the most important figures in LGBTQ civil rights history were people of colour who fought for the rights of coloured queer people, such as Marsha P. Johnson. Pride is not a hobby: it is explicitly political in nature.

Ableism

As well as failing to understand the intersection of race, sexual orientation, and gender identity, Pride fails its members who are disabled. This happens both at Pride, a once-a-year event, and in the general community events which happen year-round. An example of ableism in Pride was at the 2011 Edmonton pride parade. An article covering this topic says this: "Edmonton Pride's official slogan this year is 'STAND UP.' Although dismayed by the ableist language, we were hoping, at the very least that this slogan signalled a move towards a more political Pride" (Peers). The slogan, in fact, asked readers to "STAND UP" and dance, or to "STAND UP" and barbecue—far from overtly political activities. This erasure of disabled bodies is not unusual in Edmonton, or Canada at large. In most queer campaigning there "is the noticeable lack of fat, gender-queer, wheeling, scootering, ageing, small-statured, cane-wielding, pre-pubescent and dog-guided members of our queer communities" (Peers). When summer rolls around, "the Edmonton Pride Festival society rents one of the most accessible venues in Edmonton, and, through great expense and logistical prowess, manages to transform it into an almost entirely inaccessible space" (Peers). Most year-round events aren't any better: being held at the top of stairs, neglecting to accommodate walking assistance devices, and remaining unsuitable for people with non-normative hearing or sight (Peers). Another obvious example of this is that Pride parades themselves reinforce the ableist assumption that participants can walk: freely, easily, and without pain. All of this is indicative of an atmosphere within queer communities that doesn't include people with disabilities. Even if there is no explicit sign—like a staircase—disabled people often feel excluded from the community at large. As stated earlier in this essay, "the ideal queer person" is able-bodied, to better appeal to the non-LGBTQ Canadian audience. The LGBTQ community itself has absorbed this attitude.

Sexism

While the face of Pride is not one of the disabled body, the same can be said of women. This fact finds its origins in misogyny, of which Pride is not exempt. This cultural maligning of women reveals itself in Pride celebrating men's sexuality over women's sexuality. Women's sexuality is often a source of anxiety in our culture—it is dark, unknowable, and utterly other (Creed 1). If this is so for women's heterosexuality, it can only be doubly so for lesbianism or other sapphic orientations. This anxiety often manifests as an outright denial of queer female sexualities (Lamble 81). In Canadian history, sexually active gay men were perceived as defiant and immoral, and so the act was criminalized. In contrast, sex between women was almost never directly, legally addressed (Rau). In Canadian history and in the present, "lesbians appear as disembodied, desexualized legal subjects" (Lamble 81). An example of this in the modern world is the fact that the age of consent for oral or vaginal intercourse is 16, while the age of consent for anal intercourse is 18 (Rau). Currently, men and women who engage in same-gender sex face different levels of criminalization. This clearly shows the different ways in which queer sexualities are discriminated against based on gender. Gender and sexuality are extremely close concepts in patriarchal Canadian culture, where a seemingly intrinsic part of being a woman is desiring men.

Therefore, lesbianism is an act of subverting female gender roles in patriarchal culture. Deeply rooted cultural anxiety over female sexuality in Canadian society, combined with patriarchal expectations for female desire, culminate in the fact that male sexuality, even when it entitles men's attraction to other men, is often more palatable in our society than non-heterosexual female sexuality. This purposeful invisibility of female queer sexuality is a sign of Pride's homonormativity.

Classism

Having discussed race, gender, and ability, the final way I will discuss the shortcomings of Pride and the LGBTQ community is in relation to class. Pride should accommodate those that do not have the financial means to live a comfortable economic existence. Examining Pride through a class lens is particularly important because of the correlation between LGBTQ youth and homelessness—LGBTQ youth are more likely to be homeless than almost any other demographic (Kirkup). In Canada there are startlingly few studies done to survey the amount of homeless youth who are LGBTQ, but some researchers say that around 40-50% of homeless youth are LGBTQ (Kirkup). Another study finds that 1 in 5 Toronto homeless youths identified as LGBTQ ("Facts & States"). This is extremely disproportionate. According to Statistics Canada, only 1-1.7% of the Canadian population identifies as LGBTQ ("Same-sex couples"). These statistics would only reflect the amount of LGBTQ people who were "out." Even so, the number of homeless LGBTQ youths far outpaces the relative size of the national community. Pride does not factor this into event planning most of the time. Pride parades can be expensive affairs: from surcharges for simple attendance, expensive food vendors and merchandise, and travelling fees. I have struggled with this myself. Before Nanaimo overcame the discrimination in the city council and general population to have its first Pride parade, the only nearby major Pride event was held in Vancouver. I would have to pay for the ferry, food, and accommodations. This was expensive enough that I was never able to attend, so my first Pride was the one held in Nanaimo. One of the biggest offences related to pay-to-play culture is the Stonewall Pride march, which has been described as "a commercial extravaganza of huge proportions" (Clare). The 25th anniversary of the Stonewall riots struck many as "not so much as a celebration of a powerful and life-changing uprising of queer people, led by trans people of color, by drag queens and butch dykes, fed up with the cops, but as a middle- and upper-class urban party that opened its doors only to those who could afford it" (Clare). I'm sure it's very fun for those who can afford to go. It seems unfair, however, to limit one's engagement in queer culture based on monetary wealth, when LGBTQ youth, women, people of colour, and disabled people face significant financial barriers to participation.

How to be Proud of Pride

Having identified a number of barriers to truly inclusive Pride events, I now turn to how we might make them more welcoming to everyone in the LGBTQ community. While making Canadian Pride completely inclusive of all its members would require making the wider Canadian culture free of prejudice, this is an undertaking too large for the scope of this essay. Instead, I will focus on more achievable goals. When it comes to racism in Pride, excluding police and honouring groups such as BLM is a straightforward step. It is also important to actually listen to marginalized groups when they say something is not right, or if they have suggestions for improvements to Pride: they know more about what they need than people who do not share their lived experiences.

A way to combat ableism in Pride is to be aware of whether the venues one attends are disability-friendly or not. If they aren't, bring attention to this fact and make a fuss about it, or join the organizing committee and make sure future venues are accessible. The only way for change to happen is to push for it. Again, listening to disabled LGBTQ communities is the best way to know how to move forward.

Misogyny can be incredibly insidious. When it comes to queer women, increased visibility would go a long way towards combating the combined effects of sexism and heterosexism. I would love to see more women's events in my own community, and a greater platform for women's groups at Pride. A shift of this kind would help Pride to be more inclusive of the queer women who attend.

As for classism, one shouldn't need to be rich

to go to Pride. Surcharges for events such as Stonewall 25 should be done-away with. While I can see the need for some venues to charge for attendance if they do not otherwise have enough funds to continue offering them, a pay-as-much-as-you-can system would be incredibly beneficial. When it comes to Pride, a greater platform should be given to the homelessness epidemic the youth of the LGBTQ communities are facing. As well, more small towns and cities should have Pride events, so that people don't feel pressured to travel simply to engage in their own culture.

Pride has the potential to be an amazing source of affirmation in your own identity and community, as well as a platform for activism. However, aspects of racism, ableism, sexism, heterosexism, classism, as well as homonormativity have gained a foothold in the festivities. It is by continuing the dialogue of intersectionality within LGBTQ communities and allowing marginalized identities to have voice in these proceedings that prejudice within LGBTQ communities and the events of Pride can be combated. Only then, can we be proud of Pride.

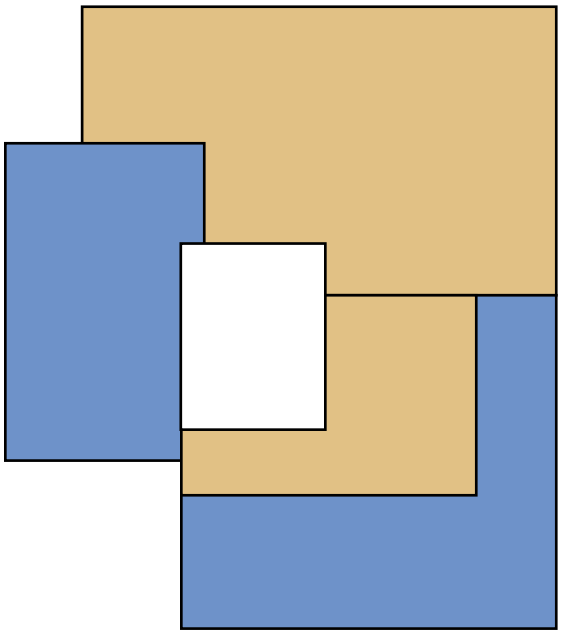

Works Cited

Born, Tyler. "Marsha 'Pay it no Mind' Johnson." Challenging Gender Boundaries: A Trans Biography Project, Out History, outhistory.org/exhibits/show/tgi-bios/marsha-p-johnson. Accessed 29 Oct. 2016.

Christopher, Nathaniel. "Nanaimo mayor won't proclaim Pride." Xtra, 20 Jun. 2007, www.dailyxtra.com/nanaimo-mayor-wont-proclaim-pride-18733. Accessed 27 Jun.2017.

Clare, Eli. "Losing home." Exile and Pride: Disability, Queerness, and Liberation. New York, 2015, pp. 31-49.

Creed, Barbara. The Monstrous-Feminine: Film, Feminism, Psychoanalysis. Routledge, 15 Nov. 1993, p. 1.

Crenshaw, Kimberle. "Traffic at the Crossroads: Multiple Oppressions." Sisterhood is Forever: the Women's Anthology for a New Millenium, Toronto: Washington Square Press, editor Robin Morgan, 2003, p. 43.

"Facts & States." Covenant House Toronto, www.covenanthousetoronto.ca/homeless-youth/Facts-andStats. Accessed 7 Nov. 2016.

Fox, Catherine O., and Tracy E. Ore. "(Un) Covering Normalized Gender and Race Subjectivities in LGBT 'Safe Spaces.'" Feminist Studies, Vol. 36, No. 3, 2010. pp. 631-633, www.jstor.org/stable/27919125. Accessed 6 Nov. 2016.

Greensmith, Cameron, and Sulaimon Giwa. "Challenging settler colonialism in contemporary queer politics: Settler homonationalism, pride toronto, and two-spirit subjectivities." American Indian Culture and Research Journal, Vol. 37, No. 2, 2013, p. 133, doi:10.17953/aicr.37.2.p4q2r84l12735117. Accessed 7 Nov. 2016.

Jamieson, Mark. "Shame on Pride and Black Lives Matter." The Star, 11 Jul. 2016, www.thestar.com/opinion/commentary/2016/07/11/shame-on-pride-and-black-lives-matter.html. Accessed 5 Nov. 2016.

Khan, Janaya. "How a Black Lives Matter Toronto co-founder sees Canada." Maclean's, interview by Zane Schwartz, 8 Jul. 2016, www.macleans.ca/news/canada/how-black-lives-matter-co-founder-janaya-khan-sees-canada/. Accessed 30 Oct. 2016.

Kirkup, Kristy. "Half of homeless Ottawa youth identify as LGBTQ." CBC, 9 Sept. 2013, www.cbc.ca/news/canada/ottawa/half-of-homeless-ottawa-youth-identify-as-lgbtq-1.1699604. Accessed 7 Nov. 2016.

Lamble, Sarah. "Unknowable Bodies, Unthinkable Sexualities: Lesbian and Transgender Legal Invisibility in the Toronto Women's Bathhouse Raid." Queerly Canadian, edited by Maureen FitzGerald and Scott Rayter, Canadian Scholars Press Inc., Toronto, p. 81.

Pastrana, Antonio J. "Trump(et)ing Identities: Racial Capital and Lesbian and Gay Organizing." Sexuality Research and Social Policy, Vol. 7, No. 2, Jun. 2010, pp. 99-101, doi:10.1007/s13178-010-0013-2. Accessed 6 Nov. 2016.

Peers, Danielle, and Lindsay Eales. "'Stand Up' for Exclusion?: Queer Pride, ableism and inequality." Canadian Federation for the Humanities and Social Sciences, 7 Jul. 2011, www.ideas-idees.ca/blog/stand-upfor-exclusion-queer-pride-ableism-and-inequality. Accessed 5 Nov. 2016.

Rau, Krinsha. "Lesbian, Gay, Bisexual and Transgender Rights in Canada." The Canadian Encyclopedia, 16 Jun. 2014, www.thecanadianencyclopedia.ca/en/article/lesbian-gay-bisexual-and-transgender-rights-in-canada/. Accessed 29 Oct. 2016.

"Same-sex couples and sexual orientation... by the numbers." Statistics Canada, www.statcan.gc.ca/eng/dai/smr08/2015/smr08_203_2015. Accessed 7 Nov. 2016.

Santora, Marc. "Last Call at Pulse Nightclub, and Then Shots Rang Out." The New York Times, 12 Jun. 2016, www.nytimes.com/2016/06/13/us/last-call-at-orlando-club-and-then-the-shots-rang-out.html?_r=0. Accessed 10 Nov. 2016.

Sheppard, Maia, and J. B. Mayo, Jr. "The Social Construction of Gender and Sexuality: Learning from Two Spirit Traditions." The Social Studies, vol. 104, no. 6, 2013, p. 262. doi:10.1080/00377996.2013.788472

Stern, Rachel. "Nanaimo Pride Society promotes inclusive community." Nanaimo News Bulletin, 12 May. 2016, www.nanaimobulletin.com/entertainment/379200571.html. Accessed 30 Oct 2016.

"Stonewall Riots: The Beginning of the LGBT Movement." The Leadership Conference, 22 Jun. 2009, www.civilrights.org/archives/2009/06/449-stonewall.html referrer=https://www.google.ca/. Accessed 29 Oct. 2016.

Wortley, Scot. "Police Use of Force in Ontario: An Examination of Data from the Special Investigations Unit." Ipperwash Inquiry, www.attorneygeneral.jus.gov.on.ca/inquiries/ipperwash/policy_part/projects/pdf/AfricanCanadianClinicIpperwashProject_SIU-StudybyScotWortley.pdf. Accessed 24 Jun. 2017.

The Silent Epidemic: Global Threat of Antibiotic Resistant Bacteria: Carbapenem-Resistant Enterobacteriaceae (CRE)

Maya Tselios, Emily Yeung
University of British Columbia, Vancouver, British Columbia, Canada

Abstract

In silico mathematical modeling and optimization has been a reliable means to predict the morbidity of diseases. Diseases associated with Carbapenem-Resistant Entero-bacteriacae (CRE) are difficult to treat and have been with high mortality rates due to the highly adaptive nature of this bacterial family. Currently, CRE is resistant to almost all antibiotics available (Chen, Todd, Kiehlbauch, Walters, & Kallen, 2016) with mortality rates of about 45% ("Vital Signs", 2013). To better evaluate the severity of CRE outbreaks in Canada and the United States (US), a Python program that analyzes and predicts the potential of outbreaks escalating into epidemics was developed. The program uses two mathematical models that compare and graph the relative amounts of individuals/patients that are susceptible, infected or dead. The first model is deterministic which involves static rates taken from various data sources, whereas the second model is stochastic, which reflects dynamic rates according to parameters like time and changes in infectivity rate. Both models predicted epidemics in Canada and the US under current conditions, as expected.

Introduction

Carbapenem-Resistant Enterobacteriaceae (CRE) are gram-negative bacteria with highly evolved antibiotic resistance mechanisms. CRE mostly owe their rapid evolution of resistance to mobile genetic elements on their plasmids that can be transferred efficiently amongst bacteria (Kumarasamy et al., 2010). The resistance arises from certain genes that code for enzymes classified as β-lactamases, which cleave β-lactams—varied antibiotic molecules that inhibit bacterial cell wall synthesis (Nordmann, Dortet, & Poirel, 2012). Moreover, the mobility of plasmid genes and frequent global travel facilitate the spread of β-lactam resistance in global bacterial populations (Kumarasamy et al., 2010). Carbapenems are often the selected treatment for severe infections by extended-spectrum β-lactamase (ESBL) producing bacteria (Muhammed, Flokas, Detsis, Alevizakos, & Mylonakis, 2017; Harris, Tambyah, & Paterson, 2015), which are resistant to newer β-lactams such as third-generation cephalosporins and monobactams (Abreu, Marques, Monteiro-Neto, & Gonçalves, 2013). However, heightened use of carbapenems eventually selects for carbapenem resistance (McLaughlin et al., 2013).

Carbapenemases are β-lactamases that inactivate carbapenems. To date, there are several carbapenemases that have been identified, the most clinically significant being KPC, NDM, VIM, and IMP types (Tzouvelekis, Markogiannakis, Psichogiou, Tassios, & Daikos, 2012). Hypothetically, if any KPC carbapenemase were expressed in conjunction with any NDM, VIM, or IMP carbapenemase, the bacterium would have additional resistance to β-lactams such as all generations of cephalosporins, and aztreonams (Nordmann et al., 2012). Furthermore, NDM-1 is prevalent in parts of India and China (Liu et al., 2015; Kumarasamy et al., 2010), and KPC-2 and KPC-3 have become endemic in China, the US, and Italy (Munoz-Price et al., 2013).

The evident risk of CRE warrants its place in the first list of antibiotic-resistant priority pathogens, published by the World Health Organization (Lawe-Davies & Bennet, 2017). It catalogues the 12 families of bacteria that pose the greatest threat to human health, including Acinetobacter baumannii, Staphylococcus aureus, and Pseudomonas aeruginosa (Lawe-Davies &

Bennet, 2017). The family of interest, Enterobacteriaceae, is categorized under 'Priority 1' (Lawe-Davies & Bennet, 2017). Bacterial families under 'Priority 1' are said to be critical threats, meaning that they often cause deadly infections, like pneumonia, and are resistant to numerous types of antibiotics, including carbapenems and third-generation cephalosporins (Lawe-Davies & Bennet, 2017). It is worthy to note that carbapenems and third-generation cephalosporins are the most effective antibiotics thus far to treat multidrug resistant bacteria (Lawe-Davies & Bennet, 2017). In addition, risk factors like the misuse of antibiotics (Bell et al., p. 11), inadequate hygiene in hospitals ("Antimicrobial Copper", 2015), direct contact with infected individuals ("Healthcare-associated Infections", 2015), touching contaminated medical equipment (Russotto, Cortegiani, Raineri, & Giarratano, 2015; Roux, Aubier, Cochard, Quentin, & Mee-Marquet, 2013), and decreased antibiotic production ("Antimicrobial Copper", 2015) would increase the likelihood of a CRE epidemic.

In 2016, a CRE isolate from a fatal clinical case was tested against all 26 available antibiotics inthe US, and was found to be resistant to all of them (Chen, Todd, Kiehlbauch, Walters, & Kallen, 2016). CRE infections have also become endemic in many countries, including the US, Greece, Brazil, Israel, and China (Munoz-Price et al., 2013). A study by Thaden et. al concluded that, in community hospitals in the Southeastern US, diagnoses of CRE increased by five times from 2008 to 2012 (2014). In a study conducted in a Greek tertiary care university hospital, the number of carbapenem-resistant K. pneumoniae infections increased from 17 cases to 96 cases between 2005 and 2014 (Spyropoulou et al., 2016). A Europe-wide assessment of 38 countries found that 13 (34.2%) countries reported increasing rates of CRE infections, 16 (42.1%) reported no change in their epidemiological situations, and 9 (23.7%) reported improvement between 2013 and 2015 (Albiger, Glasner, Struelens, Grundmann, & Monnet, 2015).

It is important to create a mathematical model that can predict a CRE epidemic under current conditions, since data suggest that an epidemic may be imminent. Current conditions include the misuse of antibiotics in Canada ("CARSSR", 2016) and in the United States (Cable, 2017) . The model will use data from the United States (US) and Canada, due to their close interaction as countries. Additionally, giving experts and medical professionals access to a predictive program would aid in slowing the already increasing global incidence of CRE. Python will be used to build this model, because in comparison to other programming languages, Python will provide a more mathematically rounded approach to the calculation of differential equations. Subsequently, these equations serve to model the spread of CRE infection and predict the consequences. However, given the epidemiology and high mortality of CRE infections, one can expect the model to predict a CRE epidemic in both Canada and the US.

Methods

The purpose of making the deterministic model, which consists of static rates, was to offer a comparison to and act as a basis for the stochastic model, which consists of changing rates. This enables us to assess the validity of the procedure, and to strengthen any conclusions. A deterministic SIR (Susceptible, Infected, and Recovered) model was created using the Python package, SciPy, which contains functions that solve and integrate the differential equations. The equations were run through the program for a calculation period of 160 months. The model consisted of eight parameters: mortality rate (g), recovery rate (rec), infection rate (b), susceptible population (S), total population (N), recovered population (R), infected population (I), and dead population (D). Mortality rate per annum was defined to be 40-50% ("Vital Signs", 2013), and we used 50% to model a worst-case scenario. The model is based on one month-intervals and thus, in the code, the monthly mortality rate was set as 0.042%. The value was derived from the yearly mortality rate. The recovery rate derived via empirical data from a study by Patel, Huprikar, Factor, Jenkins, and Calfee (2008).

Recent medical censuses performed in Canada and the U.S. ("Biggest Threats", 2016; "Canadian Antimicrobial", 2016) show that CRE infection rates are 0.2 and 0.26, respectively. For the general purposes of a model, the total population (N) in the simulation was set to be 1000, and the unit for population is in thousands. Susceptible (S), Infected (I), and Dead (D), were calculated via 3 separate differential equations, and are functions of a set of initial conditions (where I 0 = 1, as there must be one individual infected to start an epidemic; R 0 = 0, since it is impossible for recovery if infection has just started; S 0 = N - I 0 - R 0 = 999 individuals) and the infection, recovery, and death rates.

$$\frac{dS}{dt} = bSI \mid \frac{dI}{dt} = bSI - recI - gI \mid \frac{dR}{dt} = bSI - recI - gI \quad (1)$$

To construct a stochastic model, the probabilities of each parameter increase by a set value with equations based on the prior deterministic model. SciPy was used to solve the differential equations. After running both programs, graphs produced from the stochastic model were compared with those from the deterministic model. If the shapes of the graphs are similar qualitatively, the coding procedure is valid. Additionally, similar graphs would serve to further support or falsify the hypothesis.

Epidemics are characterized by a dramatic rise in infection rates, then a sharp decrease or gradual decrease ("Descriptive Epidemiology"). In this simulation, the epidemic is allowed to dissipate on its own, resulting in a gradual decrease of infection cases ("Descriptive Epidemiology"). Moreover, the model a sumes that once individuals recover, they are no longer susceptible. Therefore, the infected curve should resemble a typical point-source epidemic curve, as there cannot be another subsequent outbreak. Also, with no more susceptible individuals at the end of the simulation, all three curves will approach a final slope of 0, or equilibrium, since the number infected and dead depend on the number susceptible. The approach to equilibrium and the shape of the infected curve apply to both stochastic and deterministic models. Should the curves behave in the ways stated, then one can conclude that both models predict a CRE epidemic under current conditions.

Results

When the program was run, it produced four graphs. Figures 1 and 2 represent the models for the Canadian data. Figures 3 and 4 repr sent the American data. All curves in Figures 1-4 approach equilibrium. It is seen that in both deterministic models, Figure 1 and Figure 3, the infected curve of Canada reaches a hig er Y-value than that of the US. This also occurs in the stochastic models Figures 2 and 4.

Discussion

In order for the graphs to model a CRE epidemic, all curves must approach equilibrium, and the infected curve must resemble a typical point-source epidemic curve. All graphs produced from the simulation model the dynamics of an epidemic, because the susceptible curves (A), infected curves (B), and dead curves (C) all approach equilibrium. Curve B also resembles a point-source epidemic curve in all graphs. Thus, the deterministic and stochastic models predict epidemics in both countries. However, deterministic models of Canada and the US (Figures 1 and 3) suggest that the Canadian population comprises of more infected individuals than the United States. The same relationship can also be seen when comparing the stochastic models of the two countries (Figures 2 and 4). Taking the maxima of curve B from the deterministic models for Canada and the US, the models predict 18.3% more infections in Canada than in the US. Comparing the maxima of curve B from the stochastic models results in a 29.5% greater number of infections. These results suggest that Canada has a greater risk of a CRE epidemic than does the US.

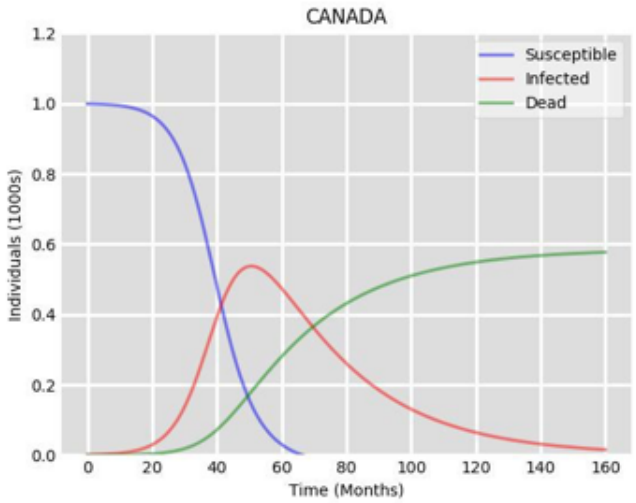

Fig. 1. This is a deterministic graph using Canadian data.

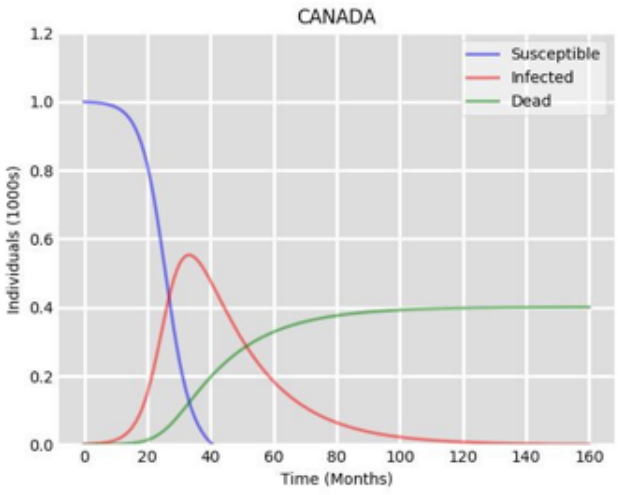

Figure 2. This is a stochastic graph using Canadian data.

This conclusion is supported by the minimal usage of of antimicrobial copper surfaces in the intensive care units (ICUs) of Canadian hospitals ("Antimicrobial Copper", 2015). ("Antimicrobial Copper", 2015). In contrast, the US has implemented antimicrobial copper surfaces ("Hospital-acquired Infection Risk", 2016), which means that American ICU patients have a lower risk of being infected. American ICUs are more prepared because CRE outbreaks appeared much earlier in the US than in Canada. Moreover, it is apparent from the disuse of copper surfaces that the Canadian medical sector has not begun to address CREs as a pertinent issue. To make matters worse, Canadians consume 6387.5 antibiotics per 1000 persons yearly (CARSSR, 2016), while Americans consume 835 antibiotics per 1000 persons yearly (6). That is, Canadians consume 7.6 times more antibiotics yearly than Americans. Together, these factors and the data explain the higher risk of a CRE epidemic in Canada.

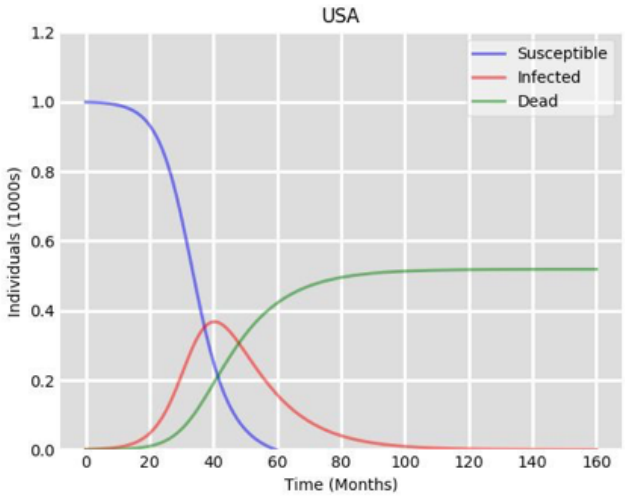

Figure 3. Deterministic graph of American data.

However, the models are not without its limitations. Specifically, the Canadian models are limited because Canada does not publish much data regarding CRE epidemiology, unlike the US. Therefore, the Canadian model would be re presentative of a few centres, but not necessarily the whole country. Nonetheless, the model serves to bring the CRE issue to light, which could inspire more research into the subject. The models also assume that after recovery, patients become immune to infection. This assumption was implemented for the sake of simplicity, though it does not take away from the conclusion, as the models still predicted epidemics while still assuming immunity. That is, models that account for reinfection would result in a similar or more grave prediction. Finally, the models do not account for conditions such as increases in sterility and antibiotic production, so the behaviour of the curves is idealized. Because of the simplicity of the model, there is no reliable way of determining quantitatively how much more at risk Canada is for a CRE epidemic. The idealisation of curves also means that no sampling was involved in the data, hence preventing statistical analysis. Nevertheless, that is not to say that the general trends produced by the simulation do not apply to reality, because the parameters were based on empirical values.

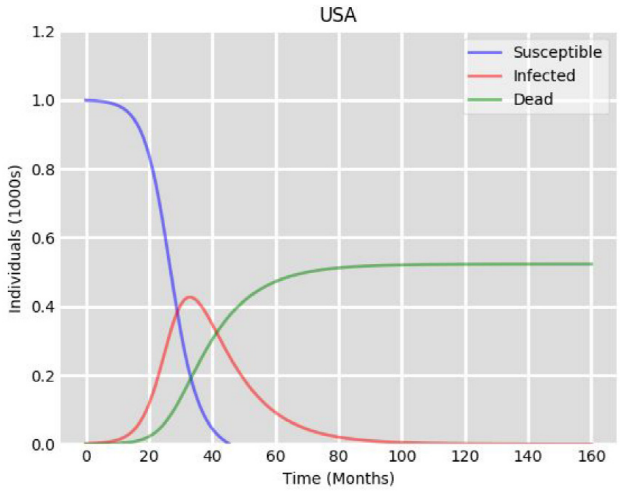

Figure 4. Stochastic model of American data. As shown, the U.S. graph approaches equilibrium much faster than the graph of Canadian data.

Conclusion

The hypothesis that CRE will become an epidemic in both the US and Canada is supported by the mathematical models. What has also been found through the model is that Canada is more at risk of a CRE epidemic. It should be acknowledged that there is still much research to be done on CRE epidemiology. Expanding data regarding CRE outbreaks in Canada is necessary to facilitate the development of better in silico predictive models. Finally, it is advised that hospitals become more vigilant when approaching hygiene and antibiotic use issues. More resources should also be put into early CRE detection techniques. Such steps are instrumental to hindering the evolution of antibiotic resistance, and minimising the risk of CRE epidemics.

PERCENTAGE OF INFECTED POPULATION AFTER ~35 MONTHS		
Country	Deterministic Model	Stochastic Model
Canada	43.4%	55.3%
US	36.7%	42.7%

Supp. Table 1. Maximum points on the Infected curve of both models for hospitals in both countries. Theses were all taken at about 35 calculated months under current conditions. The data show that Canada has more infected individuals at the epidemic's peak than the United States. Canada's higher percentage correlates with the higher misuse of antibiotics which directly contributes to the evolution of antibiotic resistance in CRE.

References

Abreu, A. G., Marques, S. G., Monteiro-Neto, V., & Gonçalves, A. G. (2013). Extended-spectrum β-lactamase-producing enterobacteriaceae in community-acquired urinary tract infections in São Luís, Brazil. Brazilian Journal of Microbiology , 44 (2), 469–471. http://doi.org/10.1590/S1517-83822013005000038

Albiger, B., Glasner, C., Struelens, M. J., Grundmann, H., & Monnet, D. L. (2015). Carbapenemase-producing Enterobacteriaceae in Europe: Assessment by National Experts From 38 Countries, May 2015. Eurosurveillance , 20 (45). doi:10.2807/1560-7917.es.2015.20.45.30062

Antimicrobial Copper Surfaces for Reducing Hospital-acquired Infection Risk [PDF]. (2016, February). ECRI Institute.

Antimicrobial Copper Surfaces for the Reduction of Health Care–Associated Infections in
Intensive Care Settings. (2015, March 31). Retrieved Match 06, 2017, from https://www.cadth.ca/antimicrobial-copper-surfaces-reduction-health-care-associated-infections-intensive-care-settings

Bell, B., Bell, M., Bowen, A., Baden, C., Brandt, M., Brown, A., . . . Wortham, J. (2013). Antibiotic Resistance Threats in the United States, 2013 [PDF]. Centers for Disease Control and Prevention.

Biggest Threats. (2016, September 08). Retrieved March 06, 2017, from https://www.cdc.gov/drugresistance/biggest_threats.html

Cable, H. (2017, March 22). Trends in U.S. Antibiotic Use. Retrieved July 01, 2017, from http://www.pewtrusts.org/en/research-and-analysis/issue-briefs/2017/03/trends-in-us-antibiotic-use

Canadian Antimicrobial Resistance Surveillance System Report 2016. (2016, September 12). Retrieved March 12, 2017, from https://www.canada.ca/en/public-health/services/publications/drugs-health-products/canadian-antimicrobial-resistance-surveillance-system-report-2016.html

Chen, L., Todd, R., Kiehlbauch, J., Walters, M., & Kallen, A. (2017). Notes from the Field: Pan-Resistant New Delhi Metallo-Beta-Lactamase-Producing Klebsiella pneumoniae — Washoe County, Nevada, 2016. MMWR. Morbidity and Mortality Weekly Report, 66 (1), 33.doi:10.15585/mmwr.mm6601a7

Descriptive Epidemiology. (n.d.). Retrieved June 30, 2017, from http://sphweb.bumc.bu.edu/otlt/mph-modules/ep/ep713_descriptiveepi/ep713_descriptiveepi3.html

Falagas, M. E., Lourida, P., Poulikakos, P., Rafailidis, P. I., & Tansarli, G. S. (2013). Antibiotic Treatment of Infections Due to Carbapanem-Resistant Enterobacteriaceae: Systematic Evaluation of the Available Evidence. Antimicrobial Agents and Chemotherapy, 58 (2), 654-663. doi:10.1128/aac.01222-13

Harris, P. N., Tambyah, P. A., & Paterson, D. L. (2015). β-lactam and β-lactamase inhibitor combinations in the treatment of extended-spectrum β-lactamase producing Enterobacteriaceae: time for a reappraisal in the era of few antibiotic options? The Lancet Infectious Diseases, 15 (4), 475-485. doi:10.1016/s1473-3099(14)70950-8

Healthcare-associated Infections. (2015, February 23). Retrieved June 29, 2017, from https://www.cdc.gov/hai/organisms/cre/cre-patientfaq.html

Kumarasamy, K. K., Toleman, M. A., Walsh, T. R., Bagaria, J., Butt, F., Balakrishnan, R., . . . Woodford, N. (2010). Emergence of a new antibiotic resistance mechanism in India, Pakistan, and the UK: a molecular, biological, and epidemiological study. The Lancet Infectious Diseases , 10 (9), 597–602. http://doi.org/10.1016/S1473-3099(10)70143-2

Lawe-Davies, O., & Bennet, S. (2017, February 27). WHO publishes list of bacteria for which new antibiotics are urgently needed. Retrieved March 06, 2017, from http://www.who.int/mediacentre/news/releases/2017/bacteria-antibiotics-needed/en/

Liu, C., Qin, S., Xu, H., Xu, L., Zhao, D., Liu, X., ...Liu, H. (2015). Correction: New Delhi Metallo-β-Lactamase 1(NDM-1), the Dominant Carbapenemase Detected in Carbapenem-Resistant Entero bacter cloacae from Henan Province, China. Plos One, 10 (10). doi:10.1371/journal.pone.0140726

McLaughlin, M., Advincula, M. R., Malczynski, M., Qi, C., Bolon, M., & Scheetz, M. H. (2013). Correlations of Antibiotic Use and Carbapenem Resistance in Enterobacteriaceae. Antimicrobial Agents and Chemotherapy, 57 (10), 5131–5133. http://doi.org/10.1128/AAC.00607-13

Muhammed, M., Flokas, M. E., Detsis, M., Alevizakos, M., & Mylonakis, E. (2017). Comparison Between Carbapenems and β-Lactam/β-Lactamase Inhibitors in the Treatment for Bloodstream Infections Caused by Extended-Spectrum β-Lactamase-Producing Enterobacteriaceae: A Systematic Review and Meta-Analysis. Open Forum Infectious Diseases, 4 (2). doi:10.1093/ofid/ofx099

Munoz-Price, L. S., Poirel, L., Bonomo, R. A., Schwaber, M. J., Daikos, G. L., Cormican, M., …Quinn, J. P. (2013). Clinical epidemiology of the global expansion of Klebsiella pneumoniae carbapenemases. The Lancet. Infe tious Diseases , 13 (9), 785–796. http://doi.org/10.1016/S1473-3099(13)70190-7

Munoz-Price, L. S., Poirel, L., Bonomo, R. A., Schwaber, M. J., Daikos, G. L., Cormican, M., …Quinn, J. P. (2013). Clinical epidemiology of the global expansion of Klebsiella pneumoniae carbapenemases. The Lancet. Infectious Diseases , 13 (9), 785–796. http://doi.org/10.1016/S1473-3099(13)70190-7

Nordmann, P., Dortet, L., & Poirel, L. (2012). Carbapenem resistance in Enterobacteriaceae: here is the storm!. Trends in molecular medicine , 18 (5), 263-272.

Patel, G., Huprikar, S., Factor, S. H., Jenkins, S. G., & Calfee, D. P. (2008). Outcomes of Carbapenem-Resistant Klebsiella pneumoniae Infection and the Impact of Antimicrobial and Adjunctive Therapies. Infection Control & Hospital Epidemiology,29 (12), 1099-1106.doi:10.1086/592412

Roux, D., Aubier, B., Cochard, H., Quentin, R., & Mee-Marquet, N. V. (2013). Contaminated sinks in intensive care units: an underestimated source of extended-spectrum beta-lactamase-producing Enterobacteriaceae in the patient environment [Abstract]. Journal of Hospital Infection,85 (2), 106-111. doi:10.1016/j.jhin.2013.07.006

Russotto, V., Cortegiani, A., Raineri, S. M., & Giarratano, A. (2015). Bacterial contamination of inanimate surfaces and equipment in the intensive care unit. Journal of Intensive Care,3 (1). doi:10.1186/s40560-015-0120-5

Shahid, M., Sobia, F., Singh, A., Malik, A., Khan, H. M., Jonas, D., & Hawkey, P. M. (2009). Beta-lactams and Beta-lactamase-inhibitors in current- or potential-clinical practice: A comprehensive update. Critical Reviews in Microbiology, 35 (2), 81-108.

Spyropoulou, A., Bartzavali, C., Vamvakopoulou, S., Marangos, M., Anastassiou, E. D.,

Spiliopoulou, I., & Christofidou, M. (2016). The first NDM metallo-β-lactamase producing Klebsiella pneumoniae isolate in a University Hospital of Southwestern Greece. Journal of Chemotherapy, 28 (4), 350-351.

Tzouvelekis, L. S., Markogiannakis, A., Psichogiou, M., Tassios, P. T., & Daikos, G. L. (2012). Carbapenemases in Klebsiella pneumoniae and Other Enterobacteriaceae: an Evolving Crisis of Global Dimensions. Clinical Microbiology Reviews, 25 (4), 682-707. doi:10.1128/cmr.05035-11

Vital Signs: Carbapenem-Resistant Enterobacteriaceae. (2013, March 08). Retrieved March 12, 2017, from https://www.cdc.gov/mmwr/preview/mmwrhtml/mm6209a3.htm

Effect of Hole Area and Incline Angle on Pipe Flow Leakage Rates

Chris Jing*, Chance Park*
University of British Columbia, Vancouver, British Columbia, Canada
* These authors contributed equally to this work.

Abstract

Water will always remain a valuable commodity due to its unique properties and availability. Therefore, its transport in pipes has great significance. Further, if leakage is controlled, an efficient mechanism of fluid administration can be created, as seen in common drip irrigation techniques. This study changed two variables of pipe perforation: hole area and pipe incline, and measured the resulting leakage rates. The experimental set-up consisted of a pipe of varying hole areas attached to a water reservoir at varying angles. We hypothesized that for a horizontally configured pipe with a single hole, the leakage rate would increase linearly with hole area. The experimental data shows consistency with the hypothesis for a certain range of hole sizes but deviates from linearity outside this range. The study also presents a novel equation that models the correlation between pipe incline and leakage rate. The findings of this study provide more knowledge to incorporate variations to the drip-irrigation technique on both flat and oblique land.

Introduction

Industrial applications

Drip irrigation is an irrigation method that works by a leakage system. The fluid flows through a perforated pipe and is deposited at desired regions on a soil surface. In certain environments, the installation of an overhead sprinkler may not be practical due to limitation in resources. For example, in an agricultural field, the drip irrigation method is a more effective way of distributing both water and fertilizer. Compared to the overhead sprinkler, the system allows for lesser evaporation of solvent with field studies finding up to 90% efficiency, with reported reduction of diseases that arise by water contact [1].

Since monoculture fields grow similar species of plants with similar affinity for water next to each other, commercialized drip irrigation systems primarily adhere to a conventional horizontal design (Figure 1).

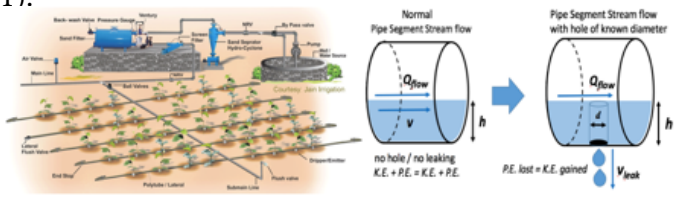

Fig. 1. (left) Typical drip irrigation system layout (figure reproduced without permission from Wikipedia [2].)
Fig. 2. (right) Side view of a pipe segment with constant flow rate Qflow, with (right) and without a hole (left).

This configuration allows for equal distribution of solvent at all points. However, fields may benefit from a non-horizontal pipe configuration, as inclined pipes deposit different amounts of leakage. Furthermore, if the land has a gradient, then knowledge about leakage rates in an angled pipe system can help distribute water to the desired amount.

Theory

Leakage from a hole of known diameter d

This experiment utilizes a horizontal pipe containing water traveling at a constant velocity (Figure 2). At the bottom of the pipe, there is a circular hole exposing the horizontal flow to a vertical channel causing leakage due to g, gravitational acceleration.

Torricelli's Law (Eq. 1), relates the velocity v_leak, of a fluid exiting a channel at the bottom of a reservoir filled to a depth h in the following form:

$$v_{leak} = \sqrt{2gh} \quad (1)$$

Since the variable at interest is the volume of leakage over time, Torricelli's law can be remodeled to give the classical discharge equation for circular orifice flow [3]:

$$Q_{leak} = k_d C\sqrt{2gh} \quad (2)$$

where Q_{leak} = leak rate (cm^3/s or mL/s)
k_d = the coefficient of discharge (*dimensionless*)
C = cross sectional area of the hole (cm^2)
g = acceleration due to gravity (cm/s^2)
h = height of the water level (cm)

The coefficient of discharge k_d accounts for energy lost from factors including boundary layer friction [4]. In the ideal condition, k_d is equal to 1.

We can solve the height of the water level h in the pipe once knowing the volumetric flow rate and the cross-sectional area of the water column. By measuring the time for a water body under a constant volumetric flow rate Q_{flow} to enter and exit a known length of the pipe segment L_{pipe}, we can compute the cross-sectional area A_{cross} of the water column:

$$A_{cross} = Q_{flow}(t_{exit} - t_{enter})/ L_{pipe} \quad (3)$$

As shown in Figure 3, the height h can then be solved analytically using geometry in two steps: First, substitute in the known radius r and A_{cross} into the equation $A_{cross} = A_{sector} - A_{triangles}$ to solve for the angle α. Next, solve the height of the water column via h=r-cos(α)r. In this experiment, the mean water height is calculated to be 0.7465 cm using this method. The height of the water column h stays relatively constant. Due to the conservation of volumetric flow rate, the leakage rate would theoretically change linearly to the area of the hole.

Inclination factor θ

The discharge equation is less accurate for predicting leakage rate when the stream is subjected to an incline. Therefore, the cross-sectional area A_cross and depth of water h must be reanalyzed.

Figure 4 shows a pipe with tube wall thickness $\boldsymbol{S}$ oriented at an angle, $\boldsymbol{\theta}$, relative to a horizontal plane. Water flows at velocity $\boldsymbol{v}$ parallel to the orientation of the pipe. The original diameter of the hole, $\boldsymbol{d}$, is equivalent to the sum of $\boldsymbol{d'}$ and $\boldsymbol{y}$. Since $\boldsymbol{y = S\ tan(\theta)}$, $\boldsymbol{d' = d - S\ tan(\theta)}$.

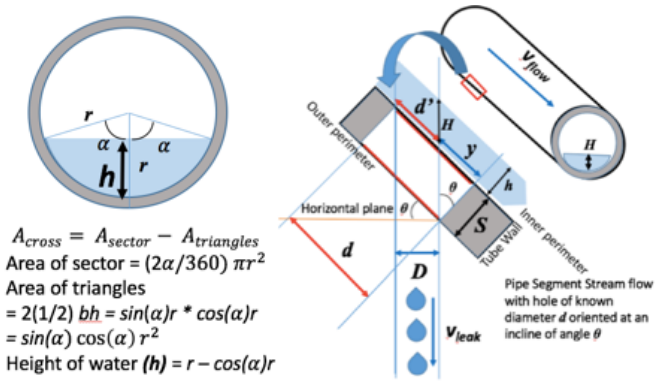

Fig. 3. (left) Cross Sectional View of Pipe and water height (h) estimation
Fig. 4. (right) Model of Inclined Pipe Leakage.

So, $\boldsymbol{D}$ is defined as the *effective diameter* in this configuration. The effective diameter is the actual diameter of the new leakage channel after the shrink in the horizontal hole size due to wall thickness and the incline is accounted for. Since $\cos(\boldsymbol{\theta}) = \frac{\boldsymbol{D}}{\boldsymbol{d'}}$, $\mathbf{D}$ can be expressed as:

$$D=\cos\theta\ (d-S\ \tan\theta) \quad (4)$$

The effective area of the hole is no longer a perfect circle. Instead, it is an ellipse of area $\pi(\frac{d}{2})(\frac{D}{2})$, , where d/2 and D/2 are the semi major-axis and semi minor-axis respectively (Figure 5).

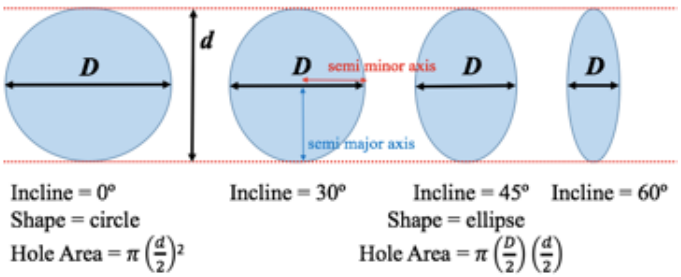

Fig. 5. The ellipse approach of effective hole area for inclined pipes.

All holes of the various inclined pipes all have the same major-axis, which is the original diameter of the hole. Their minor-axis is the effective diameter $\boldsymbol{D}$.

The height of water h in the pipe at any specific incline angle was estimated using the cross-sectional area given by Eq.3. Since t_{exit} - t_{enter} varies with angle, it becomes a variable and requires re-measurement. Similarly, the effective height of water column $\boldsymbol{H}$ replaces the perpendicular height by $\boldsymbol{H} = \frac{h}{cos(\theta)}$. Therefore, the proposed discharge equation that incorporates the structure of the inclined pipe is as follows:

$$Q_{leak} = k_e \pi \frac{d}{2} \left[\frac{cos\theta\,(d - S\,tan\theta)}{2}\right] \sqrt{\frac{2gh(\theta)}{cos\theta}} \quad (5)$$

where Q_{leak} = leak rate (mL/s)
d = actual diameter of perforation (cm)
S = thickness of tube wall (cm)
$h(\theta)$ = angle-dependent height of stream flow in the pipe (cm)
θ = angle formed between the pipe and the horizontal plane (°)
k_e = experimental discharge coefficient

Methods

Materials

IPEX Inc. SDR21 10ft PVC tubes (inner, outer diameter = 23mm, 27mm)	Stopwatch
Dura Schedule 40 PVC ¾ inch adapter	5 m (± 1mm) Industrial Measuring tape
3ft Flexible Vinyl Tubing (diameter 5/8 inch)	30cm (± 0.5mm) Steel Ruler
IPS DeWALT 20V MAX Nail gun 15 RYOBI Speed Load Nails (diameters in inches): 1/16, 5/64, 3/32, 7/64, 1/8, 9/64, 5/32, 11/64, 13/64, 7/32, 15/64, 1/4, 9/32, 5/16, 3/8	100 mL (±1mL) Graduated Cylinder The Home Depot ® Bucket
Glass Water Dispenser (2 Gallon / 7.6 L)	Step ladder
STANLEY Spirit Level	

Test facility

The experimental set-up (Figure 6) consists of a perforated pipe that is open on one end and connects to a water reservoir on the other end. The pipe connects to the reservoir via a vinyl tube, containers are placed under the hole and the open end to collect water.

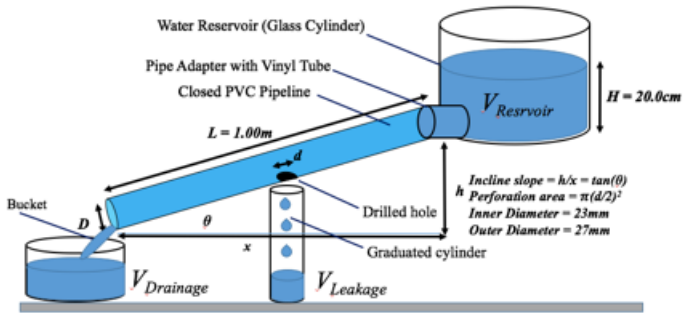

Fig. 6. Dimensional analysis of the experimental set-up. The two variables are the incline angle θ and hole diameter d.

Preparations and procedures

Pre-experimental preparations

Obtain 16 pipes of 1.00 m (± 0.01 m) length. Manually drill a single hole of known diameter at the 0.05 m mark from one end of each pipe segment. Account for any significant geometrical defects that occur inside the pipe such as residues that arise from drilling.

Place an empty reservoir on a leveled platform. Then, fill the reservoir with water until the 20.0 cm mark. Attach a faucet to the vinyl tube, the joint-adapter and the pipe in sequence. Make sure the hole on the pipe faces downward.

Experimental procedure

I. Altering hole area

Place a graduated cylinder beneath the hole to collect the leakage. Then, open the faucet and simultaneously start the timer. Close the faucet and simultaneously stop the timer when ~5 seconds have passed. Record the volume of water in the graduated cylinder. Refill the water in the reservoir back to 20.0cm high, and repeat this procedure five times to calculate the weighted mean leakage volume. Finally, repeat the procedure on pipes with different hole areas.

II. Altering pipe incline

Attach one end of the pipe to a pivot point on the table. Adjust the height of the other end of the pipe according to the desired angle, which is found using the trigonometric identity:

$$tan\theta = \frac{h}{x} \quad (6)$$

Collect mean leakages for varying hole areas. Repeat procedure for each incline.

Uncertainty propagation

Since the measurement of leak rate depends on the volume of fluid collected over a time interval in the relationship $Q_{leak}=V_{leak}/t$, the divisional/fractional uncertainty principle [5] applies as follows:

$$\frac{\delta Q_{leak}}{Q_{leak}} = \sqrt{\left(\frac{\delta V_{leak}}{V_{leak}}\right)^2 + \left(\frac{\delta t}{t}\right)^2} \qquad (7)$$

The random error associated with recording time intervals on a stopwatch is assumed to be δt = 0.11s, as determined by taking the average reaction time of the experimenter. The uncertainty in volume was estimated by half of the last digit the graduated cylinder can provide at δV= 0.5mL.

Results and Discussion

Altering hole area

As Figure 7 suggests, there is a linear correlation between the leakage rate and the hole area, suggesting a direct proportionality ($Q \propto A$) in the discharge equation (Eq. 2). After trying to minimize the chi-square value of 4.91 obtained by a one-parameter fit, a two-parameter fit that included a y-intercept was tested. A resulting lower chi-square value of 0.46 was found.

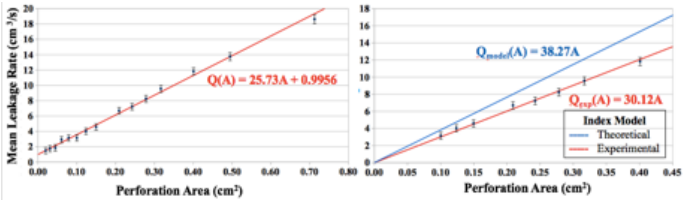

Fig. 7. (left) Mean leakage rate $\boldsymbol{Q}$ vs perforation area A for all 15 hole sizes, error bars represent relative uncertainties in $\boldsymbol{Q}$. (Red line: two-parameter fit model computed from least-square fitting with χ^2=0.46)
Fig. 8. (right) Leakage rate vs perforation area for 7 selected medium-range hole sizes, errors bars as $\boldsymbol{\delta Q}$. (Red: one-parameter fit model with χ^2=0.26; Blue: proposed linear fit from theoretical model with k_d = 1.00 and h = 0.7465cm)

However, the y-intercept that appeared in Figure 7 suggests that when the hole area is zero, leakage still occurs at a rate of 0.9956 mL/s, which is impossible. Theoretically speaking, as the hole area becomes infinitely small, there should be no water leaving due to effects such as adhesion and cohesion. Therefore, if hole diameters of a finitely small size (enough for where molecular interactions dominate) were tested, leakage rates would be expected to be zero. The linear property also deviates for oversized holes; as turbulent instability may be inevitable to the steady stream from the massive outflow of water through the hole underneath [6]. The larger the hole size, the greater the deviation would have resulted on the constant water height h inside the pipe.

Since non-extreme hole sizes are expected to follow the linear property, a second round of analyses (Figure 8) were done by including data from hole sizes between 0.1cm² and 0.4cm². χ^2 values for one-parameter and two-parameter models decreased to 0.26 and 0.11 respectively, which shows statistical significance in the model.

A further comparison between theoretical discharge slope with the experimental slope value suggests a non-ideal experimental discharge coefficient. k_e for this particular apparatus is found to be 30.12/38.27 = 0.7870 according to its definition:

$$k_e = \frac{actual\ discharge}{theoretical\ discharge} \qquad (8)$$

This value of the coefficient of discharge explains the difference found between our theoretical and our experimental linear models.

Altering pipe incline

To further investigate different properties of pipe leakage, pipe incline was introduced as a second variable. As the inclination angle increases, the relation between hole area and leakage rate becomes nonlinear.

The data taken for varying hole sizes and pipe inclines were superimposed into one graph in Figure 9, which shows the change in leakage rate at various tilting angles. There was generally a nonlinear decrease in the leakage rate as the incline slope increased. For all hole diameters tested, the drp in Q_{leak} was measured to be greatest for the smallest angle change from 0° to 4°. As the pipe becomes more tilted, the leakage rate continues to decrease but at a slower rate. The trend lines indicate that at higher incline slopes, Q_{leak} would continue its slow decreasing tendency until it approaches zero at some threshold incline when the effective hole area becomes zero. . For smaller holes, the leak-free condition occurs at a smaller incline. “8/64 inch” was the only hole diameter that has achieved this at

an angle of 20°.

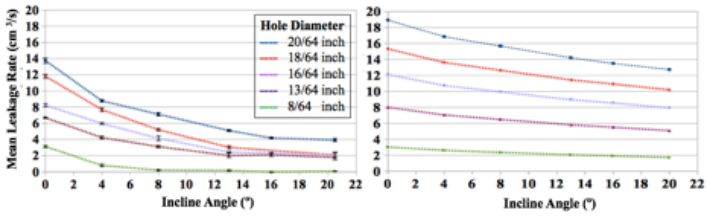

Fig. 9. (left) Mean leakage rate Q_{leak} vs Incline angle $\boldsymbol{\theta}$ for various hole-size pipes, measured at five tilting angles (4°, 8°, 13°, 16°, 20.5°), error bars represent the standard deviation from five independent measurements.
Fig. 10. (right) Predicted leak rate $\boldsymbol{Q}$ as a function of incline angle $\boldsymbol{\theta}$ for the same five hole sizes tested, based on the theoretical model of Eq. 5.

The theoretical model based on the proposed incline discharge equation (Figure 10) showed a similar decrease trend in Q_{leak} as a function of angle $\boldsymbol{\theta}$ with the greatest drop experienced in smallest angles. However, the rate of decrease in Q_{leak} is much slower from the model and suggests none of the tested hole sizes would reach leak-free standard until a very high incline angle relative to the test range. This discrepancy is likely due to the fact that the proposed model does not account for the attraction of liquid molecules to each other due to cohesion, and the attraction between liquid molecules and the inner wall of the pipe due to adhesion. This may be a large factor causing the sharp decrease in leakage rates. Therefore, the difference in the theoretical and experimental data can be explained due to the specificity of the experimental set-up; if larger holes were used, effects such as adhesion and cohesion would be minimized, and the experimental data would reflect the theoretical more accurately.

Uncertainty propagation

Error analysis in constant flow-rate assumption

The discharge equation used in the study only results in a constant leakage rate if the volumetric flow rate is constant. Since the experiment utilized a water reservoir as the source of flow, this is not the case. There is a small degree of variation that arises from the dependence of water height in Torricelli's equation. As the water leaves the reservoir and enters the pipe, the water height decreases, and the flow rate continuously decreases.

This difference was found to be negligible after an uncertainty propagation. On average, in the 5s interval that was used to collect the leakage, 0.268 L, or 2.68 x 10-4 m^3 of water left the reservoir. The reservoir had an inner circumference of 0.660 m, therefore a cross-sectional area of 0.0347 m^2. Thus, the difference in height due to the leakage would approximately be 7.22 x 10^{-3} m. By calculating the flow rates at the initial height (0.200 – 0.055 = 0.145m), and final height accounting for the decrease in height (0.145 – 7.22 x 10-3), it was found that the flow velocity only experienced a slight decrease from 1.687 m/s to 1.642 m/s as water entered the pipe over the 5s interval. This accounts for a maximum omission of 0.299mL/s of volumetric flow rate, below the 0.41mL/s minimum uncertainty of δQ.

Error analysis in perforation area

The information for the hole area in each measurement is not a result of direct measurement of the physical perforation but rather determined from the diameter labeled on each drill bit used to drill these holes prior to the experiment, which introduces uncertainty. Therefore, improving the drilling technique may ensure a more accurate hole area estimation.

Conclusion

The study has successfully found theoretical models that fit experimental data, which provide a better understanding of leakage rates when subjected to varying hole areas and pipe inclines. For an open channel pipe segment with a constant volumetric flow rate, the leakage rate for a single circular hole located at the bottom of the pipe wall was verified to be directly proportional to the area of the hole. The experimental data for leakage rates resulting from varying incline angles partially reflected the proposed incline discharge equation, but not fully, due to factors such as intermolecular interactions, which were not accounted for. Therefore, future studies should investigate the effect of increasing pipe incline angle on leakage rates with greater hole sizes (while maintaining a low hole diameter to pipe diameter ratio), where macroscopic effects dominate over intermolecular interactions.

References

[1] National Agricultural Library. "Delivery of Chemical and Microbial Pesticides through Drip Irrigation Systems." Delivery of Chemical and Microbial Pesticides through Drip Irrigation SystemsWeb.

[2] Jisl. Dripirrigation. Digital image. File:Dripirrigation.png. Wikipedia, 27 Dec. 2006. Web. 23 Mar. 2016.

[3] Swamee, P. K., & Swamee, N. Discharge equation of a circular sharp-crested orifice. Journal of Hydraulic Research, 2010, 48(1), 106-107

[4] Mannan, Sam, and Frank P. Lees. Lee's Loss Prevention in the Process Industries: Hazard Identification, Assessment, and Control. Amsterdam: Elsevier Butterworth-Heinemann, 2005.

[5] Gates, R. S., et al. "Measuring Gas Emissions from Livestock Buildings: A Review on Uncertainty Analysis and Error Sources." Biosystems Engineering. 2013, 116.3, 221-231. Web.

[6] El Khoury, G. K., Schlatter, P., Brethouwer, G., Johansson, A. V., Skolan för teknikvetenskap (SCI), Turbulens. Mekanik. Turbulent pipe flow: Statistics, re-dependence, structures and similarities with channel and boundary layer flows. Journal of Physics, Conference Series, 2014, 506(1), 012010.

Drill Bit Diameter d [inch]	Hole Radius r [cm]	Hole Area A [cm^2]	Experimental Leak Rate Q_{exp} [mL/s]	Relative Uncertainty δQ_{exp} [+/- mL/s]	Standard Deviation σ [+/- mL/s]	Model Leakage Rate Q_{model} [mL/s]
4/64	0.08	0.02	1.49	0.41	0.04	0.76
5/64	0.10	0.03	1.75	0.41	0.06	1.18
6/64	0.12	0.04	1.87	0.41	0.04	1.70
7/64	0.14	0.06	2.92	0.41	0.05	2.32
8/64	0.16	0.08	3.14	0.41	0.07	3.03
9/64	0.18	0.10	3.15	0.41	0.04	3.83
10/64	0.20	0.12	4.02	0.42	0.10	4.73
11/64	0.22	0.15	4.58	0.42	0.10	5.73
13/64	0.26	0.21	6.69	0.43	0.04	8.00
14/64	0.28	0.24	7.22	0.44	0.15	9.28
15/64	0.30	0.28	8.24	0.45	0.20	10.65
16/64	0.32	0.32	9.56	0.46	0.15	12.12
18/64	0.36	0.40	11.82	0.48	0.12	15.34
20/64	0.40	0.49	13.76	0.51	0.17	18.94
24/64	0.48	0.71	18.63	0.58	0.21	27.27

Table. 1. Experimental mean leakage rate Q_{exp} and theoretical leakage rate Q_{model} suggested by Eq. 2 for various hole sizes. Standard deviation, σ, computed over five measurements for each hole size. $\boldsymbol{\delta Q}$ established by Eq. 7